A Vascular Imaging System for Longitudinal Registration and Mapping of Superficial Vessels with Quantitative Analysis

by

Hongling Chen

B.S. Mechanical Engineering

Worcester Polytechnic Institute, 2014

Submitted to

the Mechanical Engineering Department and

the Integrated Design and Management program

in Partial Fulfillment of the degrees of

Master of Science in Mechanical Engineering

Master of Science in Engineering and Management

at the

Massachusetts Institute of Technology

May 2020

Author ....
MIT Integrated Design and Management Program (IDM)
MIT Department of Mechanical Engineering
May 15, 2020

Certified by ....
Brian W. Anthony
Principle Research Scientist, MIT Department of Mechanical Engineering
Thesis Supervisor

Accepted by..
Matthew Kressy
Executive Director
MIT Integrated Design and Management Program (IDM)

Accepted by..
Nicolas Hadjiconstantinou
Professor of MIT Department of Mechanical Engineering
Chairman, Committee on Graduate Students

(Page intentionally left blank)

A Vascular Imaging System for Longitudinal Registration and Mapping of Superficial Vessels with Quantitative Analysis

by

Hongling Chen

Submitted to the Mechanical Engineering Department and

the Integrated Design and Management program

in Partial Fulfillment of the degrees of

Master of Science in Mechanical Engineering

Master of Science in Engineering and Management

at the Massachusetts Institute of Technology

Abstract

Superficial vasculature presented on human skin is a stable and unique network across different individuals and contains important physiological information that is less understood and studied. Potential clinical applications include monitoring the progress of the peripheral arterial disease, assessment of revascularization during surgical interventions, and early assessment of skin cancer from melanoma imagery. Some non-clinical applications include biometric scanning and relocalization for ultrasound imaging. To bridge the knowledge gap between the technology and these potential applications, a reliable, robust, and versatile platform is necessary.

My thesis project involves the design and development of a platform for longitudinal superficial vasculature imaging, as well as robust computational algorithms to characterize and quantify vasculature networks. The technology used for the system includes near-infrared (NIR) optics and illumination source in the biological tissue window (750nm-940nm) optimized for hemoglobin absorption. The algorithms used, including segmentation, registration, and graph-based network analysis, are developed and implemented in Matlab. Some of my results include evidence of longitudinal vascular stability, relocalization capability, vasculature features on different parts of the human body.

Thesis Supervisor: Brian W. Anthony
Title: Principle Research Scientist, MIT Department of Mechanical Engineering

Acknowledgments

The submission of this thesis put a period mark to my three-years of life at MIT. With lots of heartfelt moments and many ups and downs, I would like to express my gratitude to many people for their support, caring and love.

First and foremost, I would like to thank my parents Yuyu Zhao and Jiuqing Chen for all their loves and supports throughout my life and my foreign journey in the US. I am incredibly lucky to receive unconditional love from both of my parents, their emphasis and beliefs in pursuing higher education and better opportunities, and their support of my many life decisions.

I would like to thank my thesis advisor Dr. Brian Anthony for his guidance, mentorship and giving me the opportunity and trust to pursue my passions.

I would like to thank all of my supportive friends from the MIT Device Realization Lab. A special thanks to Anne, Melinda, Alex, Robin, Jaffe, Rebecca, Shawn, David, Sangwoon, Shirley, Yuwei, Kai, Samatha, and Yasmin for spending many precious moments together with me and shaping my research experience at MIT.

I would like to thank Matt Kressy who saw the spark in me and thought that I belonged at MIT and belonged at IDM. I am grateful for my IDM cohort because I was constantly inspired by their bright ideas and beautiful vision of the world. Special thanks to my closest friends from IDM: Karen, Juliet, Dextina, Emily, Tanner, Shakti, Jennifer, Rachel, Susy, Pushpa, and all!

I would also like to thank Julia Wu for spending the special times together with me during the COVID-19 pandemic when I wrote my thesis. I would like to thank Anqi Tong for her support and love. I would like to thank many friends at the MIT figure skating club for the fun ice time together (best activity to relax from research work).

Table of Contents

Table of Figures

1. Introduction

1.1. Motivation

Vasculature is a network of interconnected blood vessels across all regions of our bodies. The blood vessel network is essential to support our vital daily activities as it transports blood cells, oxygen, nutrients to all body organs and tissues. Based on different functionality, blood vessels are categorized into five types: arteries, arterioles, capillaries, venules, and veins. This project studies the superficial vasculature that can be captured along the human skin without contact. This section introduces a few potential motivations for our superficial vasculature longitudinal monitoring system, and discusses current limitations of each application. These motivations are (1) peripheral vascular health monitoring, (2) biometrics identification, (3) localization for ultrasound scanning and (4) additional health information on the skin.

Superficial vascular health monitoring can be very helpful for some diseases' early diagnosis and intervention. A suitable use case of using this technology is for the early diagnosis and longitudinal monitoring of peripheral vascular disease (PVD). PVD refers to the growth of abnormalities [1] in either arteries or veins, and PVD patients usually suffer from decreased blood flow or blood clots through the blood vessel network. While PVD symptoms include leg swelling, leg pain, changes in skin temperature and texture, and red-blue discoloration of the extremities. While PVD can present in many ways, one common PVD symptom is the presence of enlarged varicose veins along the lower abdomen, pelvis, or legs as shown in figure 1 and 2. Current diagnostic methodologies for PVD patients include angiogram, ankle-brachial index, magnetic resonance angiography, Doppler Ultrasound Flow study, photoplethysmography (PPG), and most of these Methodologies are costly and not ideal for longitudinal monitoring. The superficial

vasculature monitoring technology described in this thesis can be a suitable, non-invasive, easy-to-use alternative to monitor any enlarged varicose veins change in the extremities for PVD patients. This imaging system allows for imagery of vasculature geometry and supports the reconstruction of a continuous 2D vasculature map along the extremities. The advantages of our system allow for multiple images taken at various time stamps to be overlaid in the same position for direct comparison. However, the current analysis methodology does not support a quantitative measure of venous diameter or length yet, which might be useful indicators for PVD and should be improved upon the adoption of this technology.

Figure 1 (left) - Spider veins, a mild form of varicose veins, typically appear on the legs and feet. Image source from Mayo Clinic Varicose Veins [2]

Figure 2 (right) - Varicose veins, one of the conditions of peripheral vascular disease. Image source from WebMD [3]

Other potential clinical applications for this vasculature imaging system besides PVD early detection and long-term monitoring include but are not limited to the assessment of revascularization during surgical interventions, the early assessment of skin cancer[4] from melanoma imagery, diagnosis, and monitoring on the superficial skin for hydration, perfusion condition, and any conditions reflecting on the superficial vasculature structure and skin texture (micro reliefs)[5].

The system can also be used for biometrics collection and identification as it supports imagery and re-registration. Similar to using the fingerprint as a biometric identifier, superficial vascular patterns are unique[6] across different individuals and across different body areas. The uniqueness is also validated by a study of retina vasculature from six pairs of identical twins[7] and a study of forearm vasculature patterns[5]. The fingerprint biometrics technology scans, processes, stores, reconstructs each network by their topological properties called minutiae points[8]. Other existing comparable biometric networks[9] include hand and palm geometry, retina and iris, facial characteristics have all demonstrated a consistent computational theme for using topology relationship. The vascular imaging system described in this thesis provides a reliable platform for superficial vasculature imagery across different human body locations, under the premise that an appropriate amount of vasculature appears and exists (section 2.3.2). Some parts of the body, such as the forearm, shows more apparent vasculature than others. (For discussion on the anatomical reasoning behind this, see section 1.3). This makes certain body locations more preferable and practical for biometrics scanning. Though the imaging system can be a potential scanning platform, there are some gaps between the imaging system and a biometrics identification system, including a standardized algorithm to process and categorize features and topological relationships, a standardized scanning protocol, a standardized feature parameterization guideline, and large sample size and rigorous testing.

The vascular imaging system can also be used as a localization tool coupled with other operations such as ultrasound imaging or autonomous venipuncture. Some advantageous attributes of this technology are non-invasive, visual confirmation, portability, and small form factor. The uniqueness and stability of the vasculature network make it ideal as in-vivo landmarks and the usage of localization minimally invasive than other sensing elements that demand additional coupling to the human body. Some research has shown proof-of-concept of using this technology for localization. A device for autonomous venipuncture by Chen et al [10] has

demonstrated the usability and comparable results of using this near-infrared vascular imaging technique vs. ultrasound imaging. Even though the technology has been well tested and developed, the biggest gap for application is an application-based optical design choice, calibration, and ambient lighting.

1.2.   Near-infrared (NIR) Imaging

This section introduces the near-infrared (NIR) imaging technique and explains how NIR imaging works, how it works on imaging vasculature, and how it compares to other imaging techniques for vascular imaging.

Near-infrared (NIR) imaging technique is chosen for the scope of the project because of its non-contact, non-invasive properties, and hemoglobin absorption characteristics, detailed in section 1.3. NIR imaging can be in various modes such as transmission mode, reflection mode, and the combination of the two modes. It is also usually coupled with polarizers and neutral density filters to remove the glare from the skin surface.
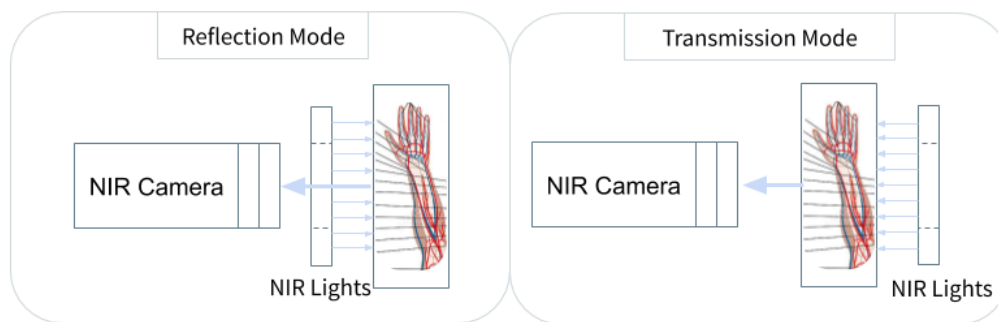
Figure 3 - Comparison between the reflection and transmission mode of NIR vascular imaging

The near-infrared optical window for the project is subjected to the NIR range of 650 - 1350nm, also referred to as the NIR-I window in some division schemes, so as to differentiate from the NIR-II window or short-wavelength infrared (SWIR) (1400-3000nm). In the following content of the thesis, the nomenclature NIR refers to the NIR-I region. Looking at the different

wavelengths in the electromagnetic spectrum, the NIR window is next to the visible window(400-700nm), however, NIR wavelength is not visible by human eyes and hence has to be captured by a camera that is sensitive to photons in the NIR region. Most consumer camera sensors are sensitive in the NIR region as long as there is no filter installed to block NIR light. More details involving the selection and specification of the NIR camera and NIR light source are discussed in sections 2.1 and 2.2.

The usage of NIR technology for superficial vasculature imaging has been well studied[11] and mostly applied in venipuncture and cannulation. Existing products of vein imaging include VascuLuminator[12], AccuVein, VeinViewer[13], and Veinsite[14] and extensive trials and studies have been conducted to compare patient cannulation results. Though the NIR imaging technology is proven to be reliable and well-developed, there has been evidence and support for longitudinal disease progression monitoring.

To study longitudinal vascular changes, NIR modality is chosen because of the benefits of non-invasiveness, the small form factor for device portability, and reasonable cost. Other commonly used modalities include ultrasound, x-ray (angiogram requires a fluorescent contrast agent), CT, and MRI. Some of these modalities may provide accurate results and even bonus benefits such as the doppler effect in ultrasound. However the difficulty of access to these machines, complexity of operations, and high cost associated accentuates the benefits of NIR imaging.

1.3.   Optical Properties of Human Skin Tissue

This section discusses the relative composition of human skin tissues and their corresponding optical properties with a focus on the hemoglobin absorption in the NIR region, and also discusses the effects of various skin tones on vascular Imaging, so as to help optimize the design of system and processing.

Light can penetrate through biological tissues such as human skin and blood mostly through scattering. NIR light (650-1350nm) has its maximum penetration depth[15] in biological tissues. Since NIR light penetrates deeper into the tissues with more effective scattering and photons travel in a longer distance, the probability of photon absorption by the tissue also increases. Light scattering properties in human skin tissues are measured by the scattering coefficient (μ_s), which is defined as the probability of the photon scattering in tissue per unit path length[16]. Figure 5 shows the scattering coefficient on human skin. However, the effective attenuation coefficient (μ_{eff})in biological tissue is driven by the transport scattering coefficient(μ_s') and the absorption coefficient (μ_a), defined as the relationship below. The absorption coefficient (μ_a) is defined as the probability of the photon absorption in tissue per path length[6][17].

$$\mu_{eff} = \sqrt{3\mu_a\,(\mu_a + \mu_s')}$$

$$\mu_s' = \mu_s(1 - g)$$

where $g = 0.9$ for the anisotropy of biological tissue

The absorption coefficient ($\boldsymbol{\mu}_a$) is the key property for vasculature imaging on human skin because different tissue components (i.e. blood and water) have different absorption under the same NIR window, hence creating a contrast between the blood vessels and other tissues.

The human skin is composed of three primary layers: the epidermis, the dermis, and the hypodermis. The most important chromophores in biological issues are blood vessels in the dermis and hypodermis, water in all layers, melanin in the epidermis, and fat in the hypodermis/ subcutaneous layer. Figure 4 below is an anatomic structure of the human skin[18].
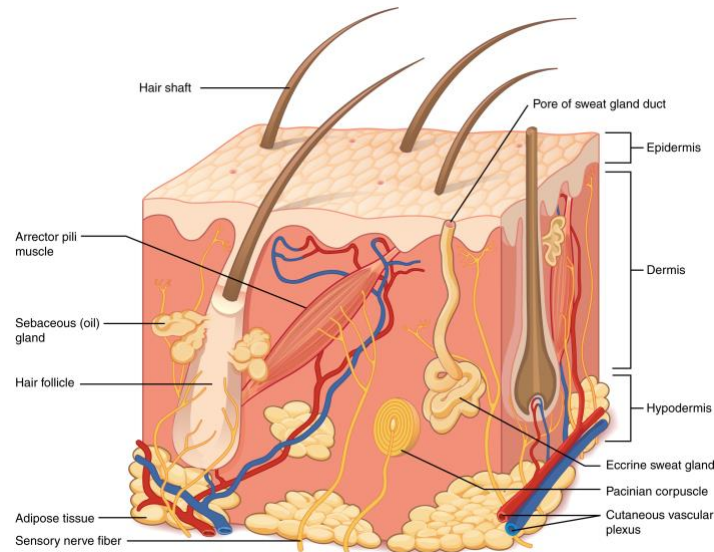
Figure 4: Layers of Skin - human skin is composed of three main layers: the epidermis, the dermis, which is composed of superficial blood vessels, hair follicles, sweat glands, and the hypodermis, which is composed of loose connective and fatty tissues [19]

1.3.1.   Hemoglobin Absorption

Blood vessels can be categorized into two different types based on the oxygenation level: veins (deoxygenated blood) and arteries (oxygenated blood). Blood contains hemoglobin(Hb), which is a protein responsible for transporting oxygen in the red blood cells of mammals. Oxyhemoglobin (HbO_2) is formed during physiological respiration when oxygen binds to the protein hemoglobin in red blood cells; Deoxygenated hemoglobin (Hb) is a form of hemoglobin unbound to oxygen. Both forms of hemoglobin absorb NIR light but contribute to different absorption based on wavelength. Figure 5 below shows the molar extinction coefficients (logarithmic representation of absorption coefficient) of HbO_2 and Hb and the spectrum range covers from visible (400 - 700nm) to NIR wavelength.
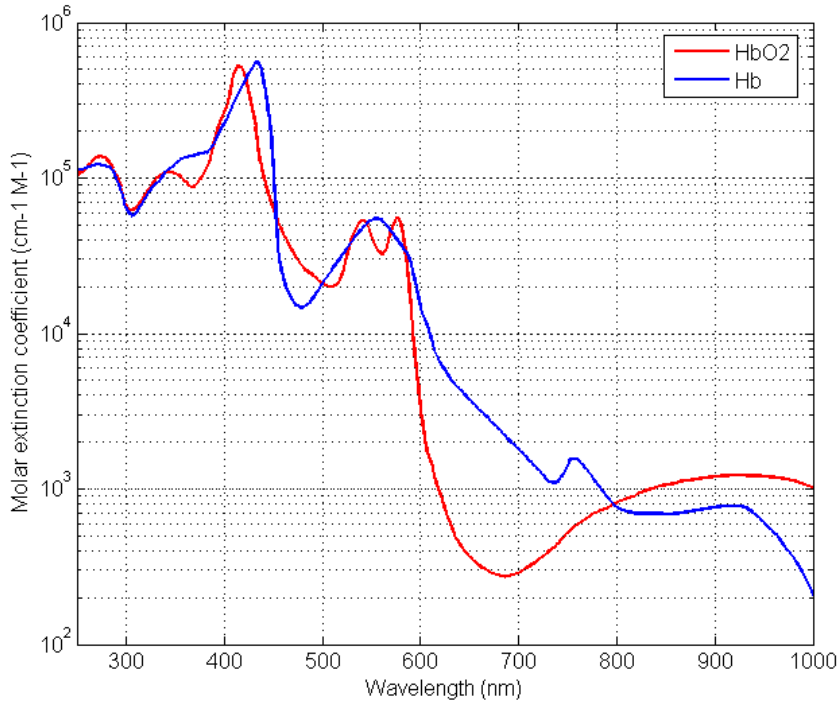
Figure 5 -The molar extinction coefficients, logarithmic representation of absorption coefficients, of HbO2 and Hb. [17, p.] Zhun310 / CC BY-SA (https://creativecommons.org/licenses/by-sa/3.0)

Water is the major component in biological tissue and also absorbs NIR light. Figure 6 below shows the absorption spectrum of water, in contrast to spectra for veins. Compared to blood at 880nm, the absorption of water is an order of magnitude lower and the effective attenuation coefficient at this wavelength is dominated by the blood absorption. Therefore, imaging using NIR light can create a significant contrast of absorption between blood and all other components in the biological tissue.
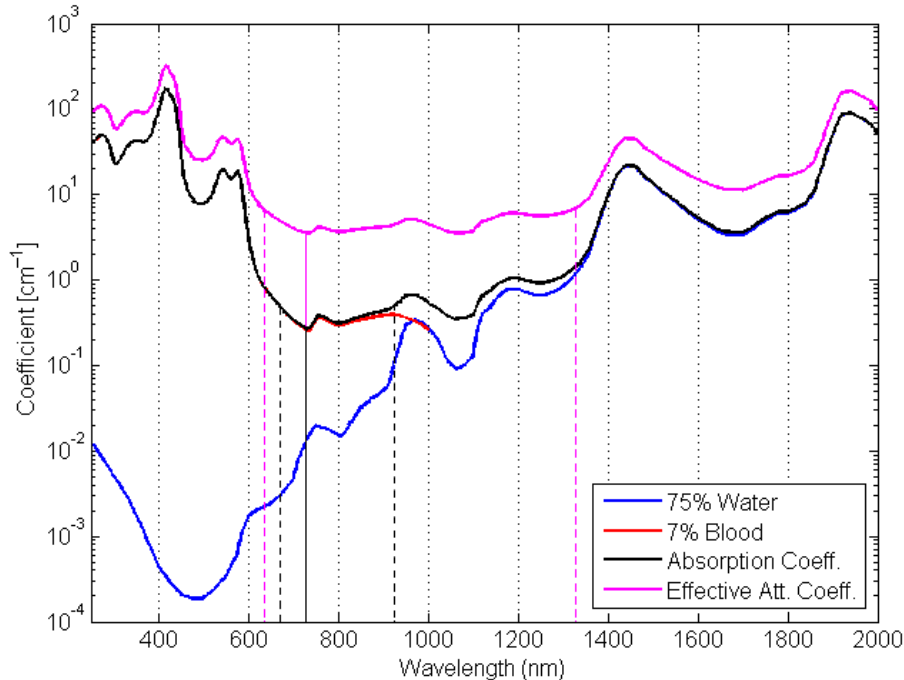
Figure 6 - Spectra for veins (SvO2 ≈ 60%).

Absorption coefficient: λmin = 730 nm; NIR window = (664 - 932) nm.
Effective attenuation coefficient: λmin = 730 nm; NIR window = (630 - 1328) nm. [17, p.]
By Zhun310 at English Wikipedia, CC BY-SA 3.0
(https://commons.wikimedia.org/w/index.php?curid=20067192)

Melanin is a chromophore that absorbs NIR light in human skin tissues. Melanin is produced by melanocytes, which are located at the bottom of the epidermal layer of the skin (see figure 7 below). Melanin can protect the skin from harmful UV radiation, and exposure to UV radiation also stimulates the keratinocyte and melanocytes to produce more melanin. Additionally, melanin is also responsible for skin pigmentation such that when sun exposure increases, the skin color generally becomes more tan. Likewise, the amount of melatonin is also correlated with skin tone. Lighter skin individuals produce less melanin than those with darker skin color. Hence the variations of skin color also have slight effects on the absorptions of NIR light, and affect the vasculature imaging quality and image contrast.
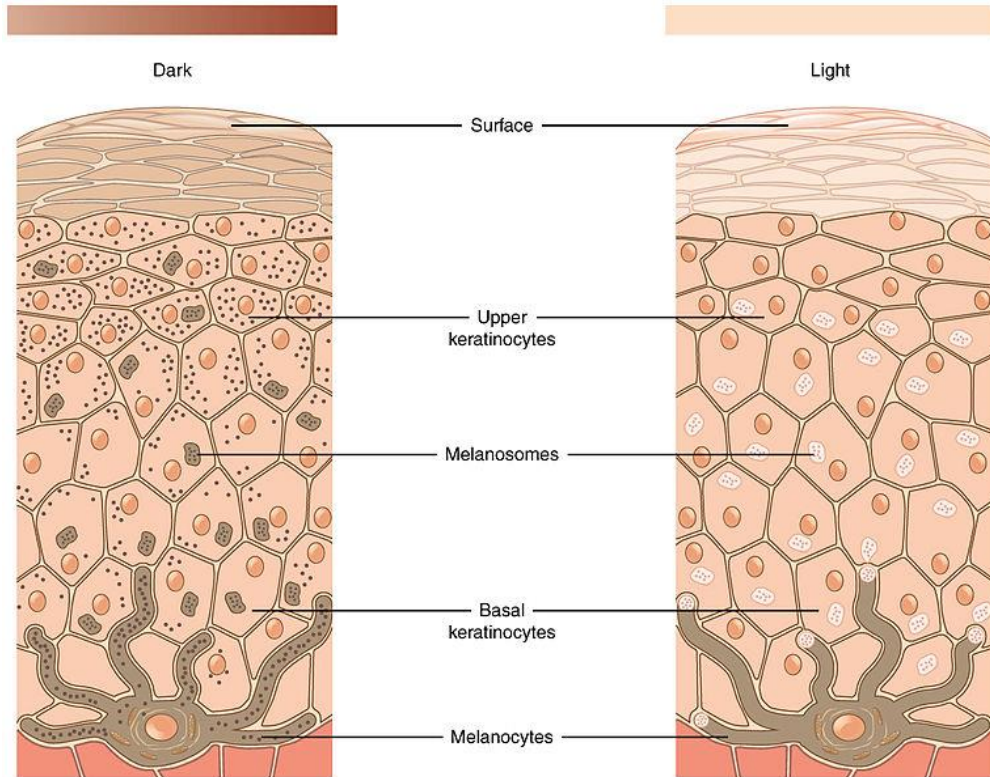
Figure 7 - Skin Pigmentation: The relative coloration of the skin depends on the amount of melanin produced by melanocytes in the stratum basale and taken up by keratinocytes.[20]

There are two types of melanin in human tissues[17]: eumelanin appearing as black-brown and pheomelanin appearing as red-yellow. The absorption coefficient of melanin in the NIR window is significantly higher than blood and water, as shown below in both forms of melanin. Therefore, melanin, or other melanocyte related components such as moles, are usually more visible on the NIR imaging.
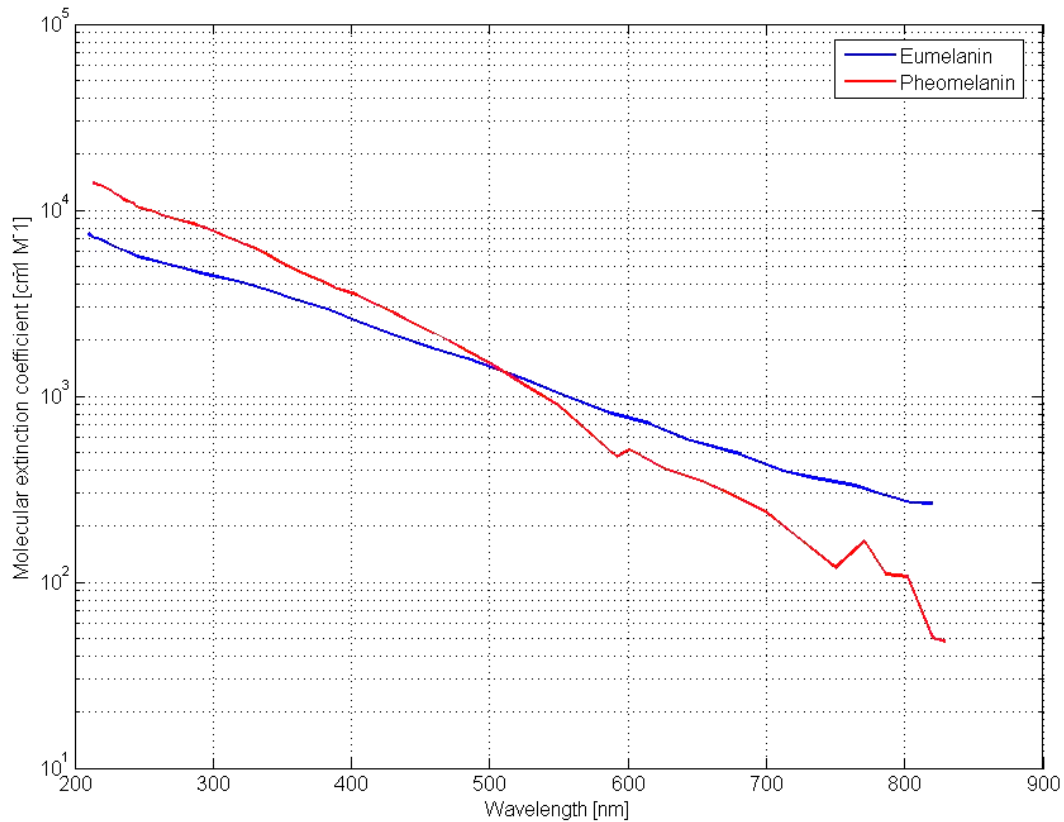
Figure 8 - Molar extinction coefficients of eumelanin and pheomelanin

Zhun310 / CC BY-SA (https://creativecommons.org/licenses/by-sa/3.0)
(Extinction Coefficient of Melanin, n.d.)

Lipid, also known as fat, is stored in the hypodermis (also called subcutaneous layer or superficial fascia) layer, where it is below the dermis layer and connects the skin to the underlying fascia[19] (fibrosis tissue) of the bones and muscles. Figure 9 shows the porcine absorption spectrum. The absorption coefficient in fat within the NIR window is relatively lower than that of blood vessels.
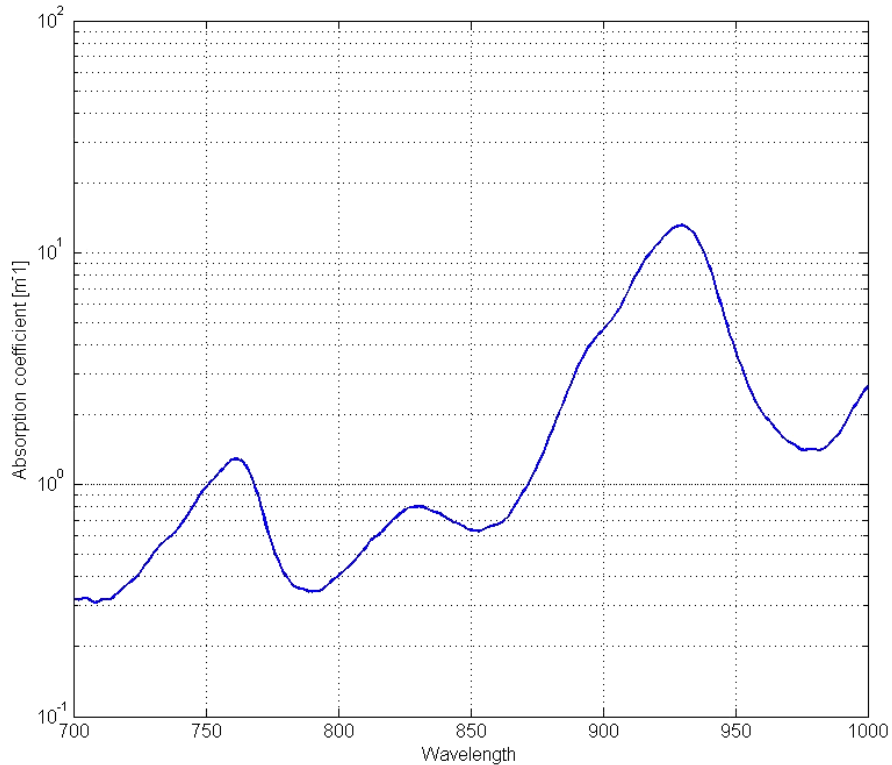
Figure 9 - The absorption coefficient spectrum of fat

1.4.   Thesis Scope

Some vasculature research work has been done by Ina Kundu Benjamin and my advisor Brian Anthony prior to 2018, which built the foundation for my thesis project. The previous work includes a portal handle device design for superficial vasculature imaging using NIR imaging technology, and some work in image processing, image segmentation, and stitching.

My thesis is to build upon previous knowledge and develop a device optimized for longitudinal vasculature imaging, as well as more accurate, reliable, and robust processing methods, quantitative analysis, and mapping. The outline of my thesis work is laid out in the chart below.
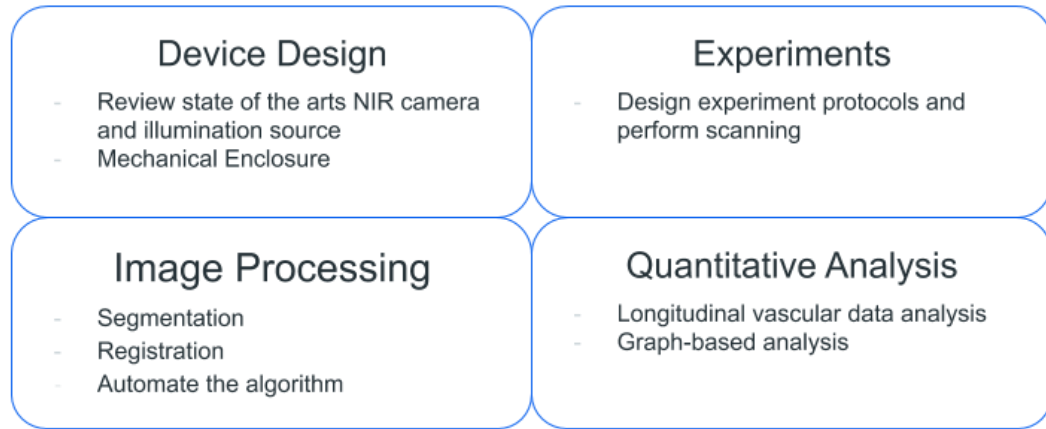
Figure 10 - Thesis Work Structure

2. System Design & Development

The superficial vasculature along the human skin can provide many important clinical and biometric information as discussed in section 1.1. Some clinical applications include cardiovascular disease monitoring (i.e. peripheral vascular disease progression), revascularization for an interventional procedure, skin pigmentation monitoring (i.e. moles, melanin), relocalization integrated with other medical systems (i.e. ultrasound, venipuncture) and some non-clinical applications include biometric identification. To achieve any of these potential applications, the aim is to design and develop a reliable platform for longitudinal vasculature imaging, registration, and mapping. Therefore, hardware development and computational analysis are both essential for this project.

The focus of chapter 2 is on tangible device design and development including a discussion of the NIR camera, NIR illumination selection, ergonomics of the enclosure design, and overall system characterization. The development process has been iterative and updated upon learning of the image processing algorithms and analysis (details in chapter 3).

The design requirements for the system are driven by the goal of establishing a reliable platform that enables longitudinal vasculature imaging, registration, and mapping. The optical

requirement is to maximize the image quality for NIR vasculature imaging, and the hardware requirement is to optimize the mechanical and system design to be robust and easy-to-use by both the operator and the imaging subject.
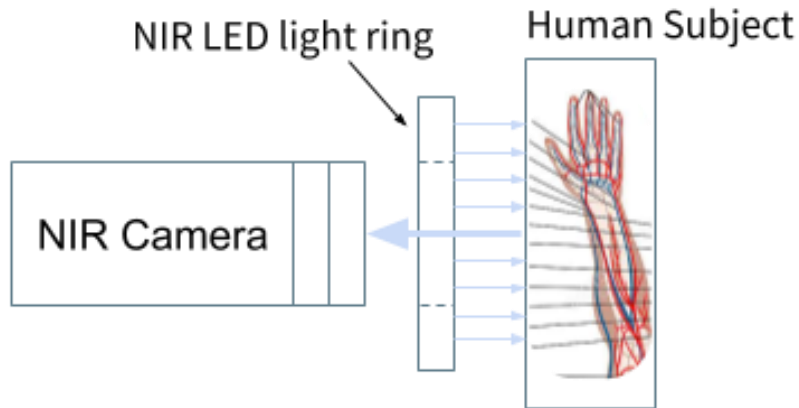
Figure 11 - Illustration of the device setup and scanning process

2.1. Camera selection

Camera selection is the most important element because the quality of raw images directly affects the quality of segmentation, registration, and analysis. The chosen camera should fulfill these requirements: (1) optimized for hemoglobin absorption, (2) high contrast between blood vessel tissues and hemoglobin, and (3) clean capture for vasculature features.

Based on the overarching imaging requirements, the selection consideration is narrowed down to some of the following specifications: NIR enhanced camera, the spectral response at hemoglobin absorption range(details in section 1.3), resolution, pixel depth, cost, form factor, weight, data transmission speed, and support for SDK development. A NIR enhanced camera is necessary because it provides the optimal imaging sensitivity (at least 30%) in the NIR window (850nm - 940nm) to highlight the tissue contrast between water and hemoglobin. Regular RGB cameras (with Bayer color filter) or RGB-modified NIR cameras (Bayer filter removed) are not suitable for vasculature imaging because it either blocks out NIR light or is mostly optimized for the visible RGB region and tends to have low quantum efficiency at 850nm. Quantum efficiency

is defined as a percentage measurement of an imaging device to convert light photons into electrons, or a sensors' electrical sensitivity to light. Spectral response is a mapping of a sensor's quantum efficiency at various wavelengths. Three NIR cameras, as shown below in figure 12, were considered based upon commercial availability and optimal specification overall. The CCD sensor SONY ICX285 significantly outperforms the CMOS CMV2000 and CMV4000 at the range from 800nm - 1000nm. Two cameras with different spectral responses, Manta G145-NIR and Mako G-419NIR were tested and the testing results echoed with the quantum efficiency specification, and it was determined that the quantum efficiency of 25% at 800nm does not provide good vascular contrasting raw images. Thus, the empirical raw image quality, as well as other factors mentioned at the beginning of the paragraph, has led to the decision of Manta NIR camera (MANTA G-145, Allied Vision, Stadtroda, Germany) for superficial vasculature imaging. The lens used is a 1X C-Mount Mitutoyo lens from Computar (model M1620-MPW2).
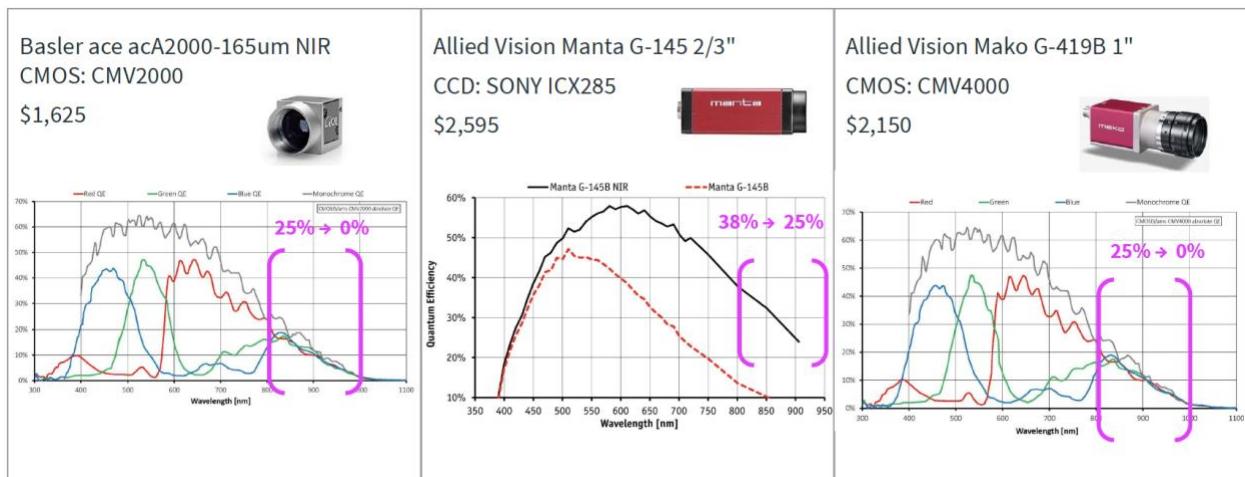
Figure 12 - Quantum efficiency comparison between the three commercially available NIR cameras in the NIR region 800-1000nm for hemoglobin absorption imaging: Basler acA2000, Manta G-145 NIR, Mako G-419 NIR. [21] [22] [23]

2.2.   Illumination

The illumination source is as important as camera selection because the imaging quality is also directly impacted by appropriate lighting in order to enhance the vasculature and provide clean and contrasting images for segmentation, registration, and analysis. The illumination source should fulfill these requirements: (1) optimal wavelength for hemoglobin absorption and vascular contrast, (2) uniformly illuminated and diffused, (3) allow for intensity adjustment, and (4) be non-invasive.

The physiological property of hemoglobin absorption and vascular contrasts (section 1.3) dictate that the NIR window 800-950 is the only appropriate region. Light distribution pattern directly affects both the illuminance scattered through the skin and the hemoglobin absorption distribution across the vasculature in the same region of interest. Non-uniform lighting may induce halo patterns, hotspots/vignettes, or other undesired optical ripple effects, in which circumstances the illumination should be diffused. It is important to have known characteristics of the illumination source such that any ripple effects can be accounted for during image processing.

Light intensity adjustment is necessary for imaging vasculature from various skin tones (section 1.3) because light reflection and absorption ratio differs across various skin tones. Empirically, imaging lighter skin tone uses lower light intensity, and imaging darker skin tone uses higher light intensity. For lighter skin tones, reflectance becomes more dominant; while for darker skin tones, a greater amount of illuminance is needed for enough absorption effects beyond the skin melanin absorption. As shown in figure 13 below, vasculature visibility and contrast are different between different levels of skin tone or melatonin concentration. Hence it is important to be versatile in the fine-tuning of illumination and optical settings.
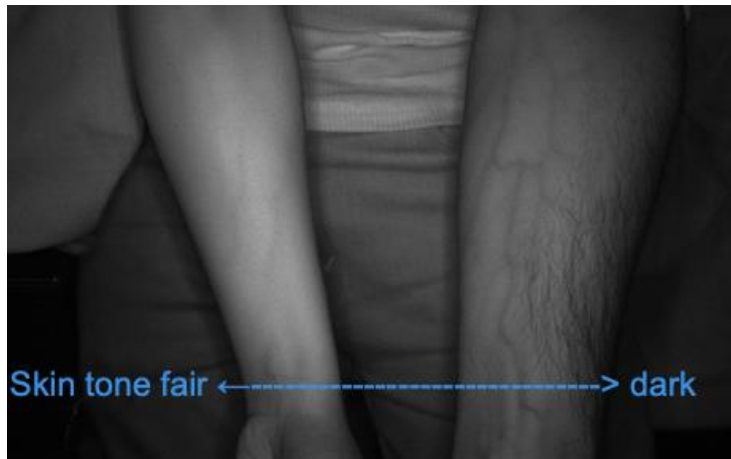
Figure 13 - Vasculature visibility comparison from different skin tones under the same illumination and optical settings

The illumination source should also be non-invasive, and minimize any photobiological risks for human tissues. NIR lights are also a large component of sunlight; although invisible, the recommendation is to avoid direct exposure to human eyes.

Given all the requirements above, a commercially available NIR LED ring is advantageous because it offers uniform circular light distribution and small form factors for device fitting. Most of the commercially available NIR light rings are at the wavelength of 850nm, 880nm, and 940nm for night vision security cameras. The decision of illumination source settles down to be NIR LED Ring Light at 880nm (Medium Aimed Bright Field RL4260, Advanced Illumination, Inc. Rochester, VT, USA).

2.3. Device Design and Development

This section discusses the mechanical enclosure design for the imaging system, the experiment setup, and the scanning process. To align with the goal of designing a longitudinal vasculature imaging system, the device should fulfill these requirements: (1) all-in-one integration, (2) be handheld, (3) have adjustable lens focus and illumination distance, and (4) ergonomics with the appropriate form factor.

2.3.1. Enclosure Design

The mechanical enclosure is designed as an all-in-one piece that incorporates the camera and illumination source (NIR LED light ring), and allows for tabletop sliding and sitting without tipping. The enclosure is designed with countersunk holes to mount the camera invisibly via M3 machine screws. The LED light ring is aligned concentrically with the camera and mounted by using three M4 machine screws distributed equilaterally self-pushing against the enclosure. The enclosure square base design allows the device to be sliding on any flat surface for non-handheld usage and stabilized image capturing; its cross-section (100mm x 100mm) allows for an ergonomic handgrip. The hollow square base is also aimed to minimize overall weight during handheld operations. The enclosure is 3D printed in ABS material with smooth surface finishing and some easy-to-grab texture for hand-holding. For future iteration, cable relief can be integrated into the mechanical housing design.

Figure 14 Enclosure Design and Assembly. The image on the left side shows CAD design with a transparent view of fittings. The middle image shows a concentric alignment between illumination distribution and camera ROI.

The image on the right side shows the horizontal adjustability of the light ring to achieve optimal light distribution distance.

2.3.2. Scanning Process

Proper scanning of vasculature is critical to ensure image quality for registration and analysis. The design of experiments took into consideration uncontrollable variables (individual's vasculature, scanning environment, ergonomics) and control parameters (camera and illumination settings). Some skin preparation work includes the use of alcohol wipes to clean the

skin surface, and removal of body hair on the scanning location if necessary (disposable razors provided). The scanning environment shall be indoor under stable ambient lighting, and any background objects in the ROI shall be removed. The number of raw images captured varies based on vasculature features and surface areas of the body; for example, for a forearm scan, the number of capturing ranges from 5-25 images. The raw images are in grey-scale because the NIR camera is monochrome and the NIR light source is invisible to human eyes.

The scanning process can be broken down to the following 5 steps:

❖ Preliminary inspection based on an individual's vasculature condition
❖ Physical alignment to ensure ergonomics and stable device setup
❖ Camera SDK setting to enhance image contrast
❖ Optical adjustment to optimize image quality
❖ Capture and save in sequence for registration reference

01	Preliminary Inspection	• Skim through vasculature location, vasculature contrast, overlapping features • Remove background objects
02	Physical Alignment	• Human subject rest the body parts (i.e. forearm) • Align the device to ROI • Device sitting on flat surface or held by the operator • Ensure comfort and ergonomics
03	Camera SDK Setting	• Set exposure and gain to optimize vasculature contrast
04	Fine Adjustments	• Adjust camera focus • Adjust illumination distance and intensity • Ensure raw image quality
05	Capture and Save	• Capture images at long-exposure • Notate the sequence

Figure 15 - Scanning Process in Detail

Overlapping vascular features are essential for registration as the scanning process is freehanded and no other localization reference is provided. Sufficient features include loops, spurs, junction branch, bifurifications[8], arches, as shown below in figure 16 insufficient features include straight line, disjointed path, and lines distorted by curvature.
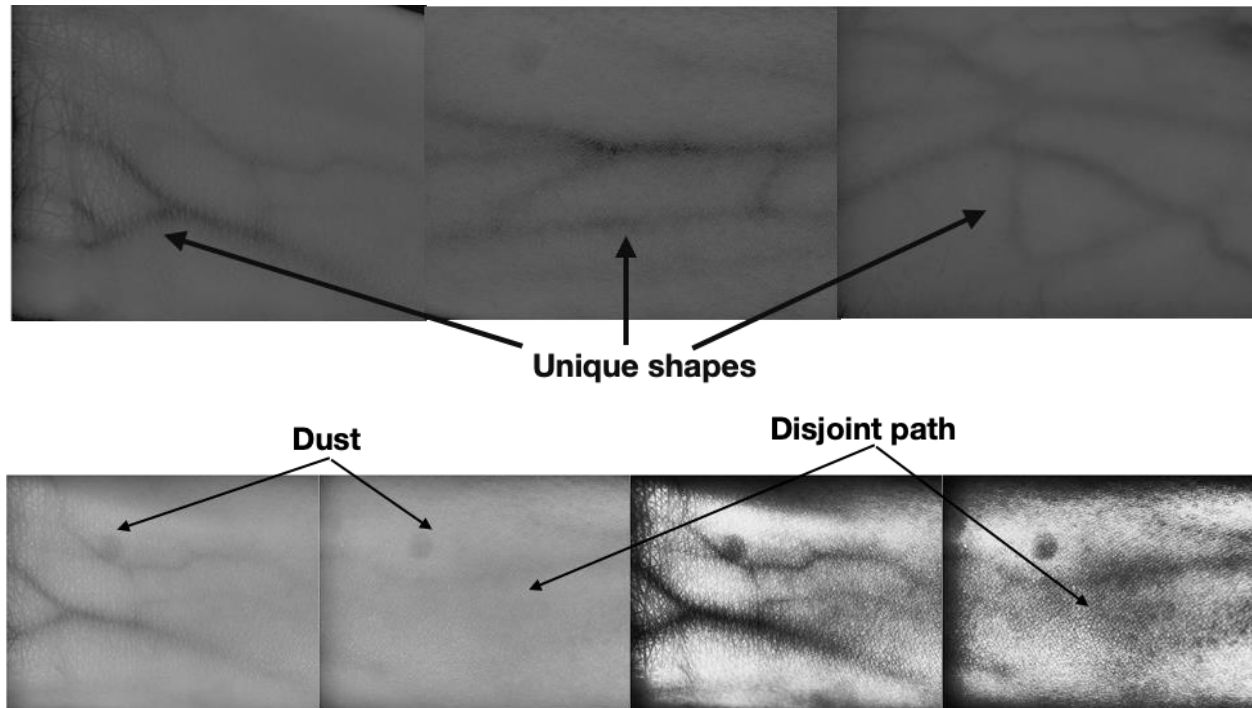
Figure 16 - Examples of Unique Vascular Features and Non-ideal Conditions.

On the bottom image, from left to right, image 3 and 4 are from the same frame as image 1 and 2 but with high contrast, effects to demonstrate any vascular features. Image 2 was the next frame of image 1 from the same scan, the vasculature path in image 2 and 4 are clearly shown as disjointed, this makes the frame problematic for registration and analysis. Artifacts or dust as shown in all frames should be avoided because these shades could be picked up as misleading point features and become problematic for registration.

To maintain ergonomics and minimize fatigue, it is highly encouraged to find comfortable resting locations for the human subject and the operators, as the scanning process requires stationary imaging capturing due to long exposure times and linear movements.

Camera exposure is defined as the amount of light per unit area reaching the sensor, measured in lux seconds, and determined by shutter speed, lens aperture, and scene luminance. Exposure time is the variable to control the shutter speed via camera SDK (Vimba Viewer, the

software from the Allied Vision). Exposure time is manually set between 15,000us - 30,000us for superficial vasculature NIR imaging.

Camera gain represents the amplification of the electrical signal from the camera sensor. For the Manta G-145 NIR CCD camera, the gain is manually controlled to optimize vasculature image quality.

2.4. System Characterization

The system is characterized by components used, optical performance, illumination distribution, mechanical measurements, and data output, as shown in the table below. One of the most advantageous characteristics of this system is the highly adjustable working distance and lighting distribution, which makes it suitable and useful in many clinical or research settings.

Components	
Sensor	Sony ICX285 CCD
Camera	Manta G-145 NIR
Lens	C-Mount M1620-MPW2
Illumination	NIR light ring RL4260
Optical Performance	
Resolution	1388 (H) x 1038 (V) or 1.4MP
Field of View @300mm	168mm (H) x 126mm (V)
Working Distance	200-600mm
Focal length	16mm
Shutter Mode	Global
Pixel Depth	12 bit
QE @ 529nm	54%
Exposure Control	0 to 33 dB; 1 dB
Gain Control	43 µs to 60 s; 1µs
Illumination @300mm working distance	
Irradiance	15.5 W/M2
Illuminance	2.6 kLux
Illumination Area	30,790 mm^2
Mechanical Specification	
Overall Dimensions	16cm x 10cm x 10cm
Weight	666g / 1.47lb
Output	
SDK	Vimba Viewer
Data transmission	GigE

The constraints of the system are: (1) each scan requires calibration due to highly customizable parameters, (2) inconsistent vasculature results between individuals, and (3) lack of measures to control angular misalignment.

Each scan, defined as a continuous capturing along the same part of the body on the same individual, requires adjustments of the camera working distance, lens focusing, and placement of the device. The design choice of having highly customized optical settings is a tradeoff between optimized vasculature contrast and the benefits of having a one-time calibration and consistent image quality. The alternative solution to address this problem while retaining the versatility is to offer fixtures at certain increments to adjust working distance and subject placement in an easy manner, rather than heavily relying on the operator's visual feedback.

Vasculature results (section 3.4) are analyzed and represented as a graph-based network with many connected nodes. Inconsistent vasculature results happen among different individuals due to the variance of human anatomical compositions, such as vasculature proximity near the skin surface level, vasculature diameter (correlates to amount of blood flow), and the ratio between hemoglobin and tissue melanin. On some individuals, the vasculature geometry may appear disconnected as a result of potentially deeper veins (>2cm). Disconnected vasculature presents challenges for registration and also results in disconnected graphs. These anatomical variants showed limitations of the NIR imaging technology used on superficial blood vessels. On the positive side, the technology is promising for longitudinal health monitoring on an individual basis because the results are reasonably consistent on the same subject and on the same part of the body.

Angular misalignments during the scanning process can cause disruption of registration or re-localization. A large angular motion may produce unmatched features from different viewing angles. The current operation mode is completely free-handed and could likely be the reason that introduces unwanted rotation. The problem can likely be addressed by either providing mechanical-assisted fixtures to limit the amount of movement or adopting some other external location reference system, such as IMU sensor, 3D scanning techniques.

3. Methodology

After capturing vasculature images, these raw images need to be processed and analyzed in order to extract useful information. This chapter describes the process and various methodologies used for vasculature image processing, relocalization, and analysis. Since the research motivation of enabling a reliable platform for longitudinal vasculature monitoring, the data processing should be automated, robust, accurate, and versatile with different subjects/locations and environments. Compared to previous analysis capability (section 1.5), the novelty of my data processing comes from clean segmentation, accurate registration, quantitative analysis, graph-based network characterization, and reconstruction. The processing steps are described in figure 17 below. All the data processing algorithms and implementation are in MATLAB 2020 (MathWorks, Natick, Massachusetts, USA).

Process Overview

➔ Raw image

➔ Pre-processing (enhancement, distortion correction, ROI)

➔ Centerline extraction & binarization

➔ Feature detection & extraction

➔ Geometric transformation & registration or re-localization

➔ Morphological processing

➔ Graph-based vascular characterization & reconstruction
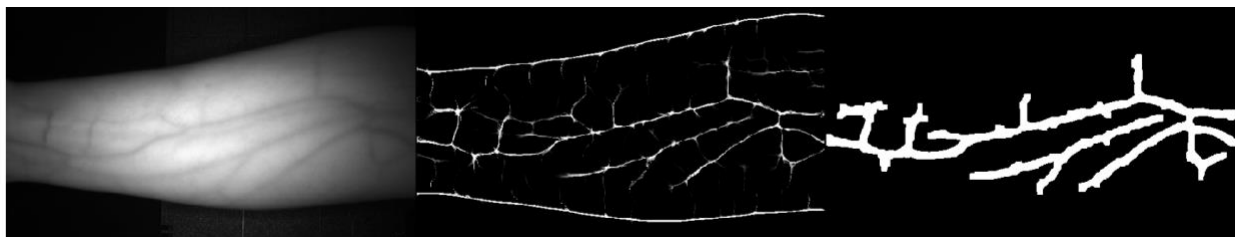
Figure 17 - Brief overview of results from raw image acquisition, centerline extraction and skeletonization

3.1.   Segmentation

Segmentation in image processing refers to partitioning an image into multiple parts or regions based on the characteristics of the pixels (i.e. similarities and discontinuity in color or shapes). Commonly used segmentation techniques are thresholding, clustering, edge detection, and more recently deep-learning-based semantic segmentation. Segmentation can be fully automated, hybrid, or manually annotated. The segmentation techniques I used, optimized for vasculature processing, leverage both color (gray-scale pixel intensity) and shape (edge detection) information and integrate techniques such as thresholding, morphological processing, and maximum curvature methods.

The goal of segmentation is to extract accurate and clean vasculature geometry and generate appropriate binarization or skeletonization, in order to successfully perform registration and graph-based analysis. Depending on the raw image quality, some images require pre-processing, but oftentimes, pre-processing is not necessary because the centerline extraction algorithm is sufficiently robust and image contrast does not affect the result.
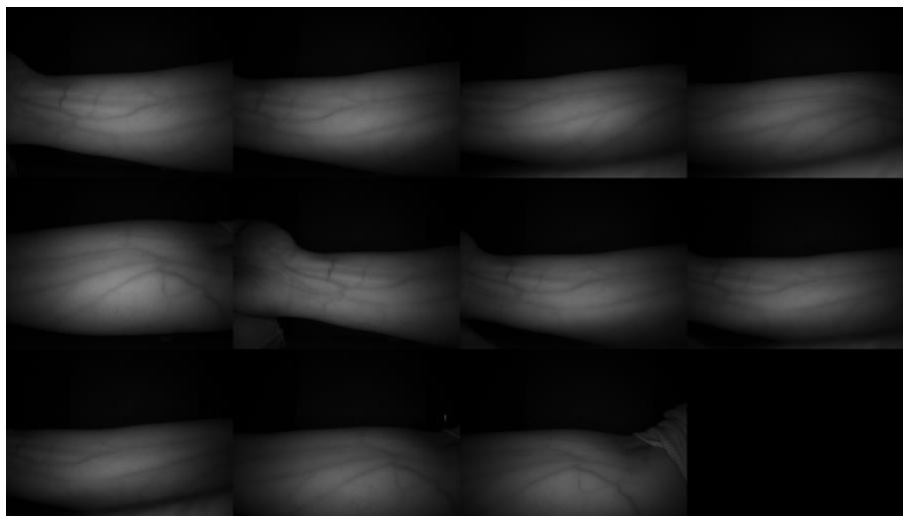
Figure 18 - A compilation of raw images from a forearm scan

Pre-processing Steps

1) Flat-field gaussian filter

2) Histogram equalization

3) The Difference of Gaussian filter

4) Median filter

5) Image crop and local graph cut (grabcut)

1) To remove hotspots or correct inhomogeneous intensity, which appears as non-uniform illumination, the flat-field[24] Gaussian smoothing technique is used with a standard deviation of sigma.

2) To improve image contrast for human perception, the histogram equalization technique is used by computing the probability of pixel intensity levels (0-255) and normalizing it to a wide-spreading distribution.

3) To highlight vascular edges and shapes, the Difference of Gaussian (DoG) technique can be used by performing a subtraction between two blur images, each obtained by convolving the original image with Gaussian blur kernel at different sigma. The DoG filter is essentially a band-pass filter that suppresses high-frequency spatial information and enhances the features within the preserved frequencies of the two blurred images.

4) To remove noise or speckles from the raw image, the Median filter is used. The median filter is a nonlinear, neighboring-based kernel that goes through all pixels and replaces each pixel value with the median value of the surrounding pixels. It's more ideal for noise reduction than linear filters such as the moving average filter.

5) To remove undesired background or blank space, an image can be cropped by chosen region of interest (ROI) or manually masked by using local graph cut[25]. The local graph cut method in the MATLAB segmenter app allows you to manually identify the foreground

and background, and automatically partition out the regions based on the image contents. The local graph cut function is great for one-time, high-contrast segmentation to remove undesired background or space. However, it is not suitable for vasculature segmentation or high-volume segmentation.
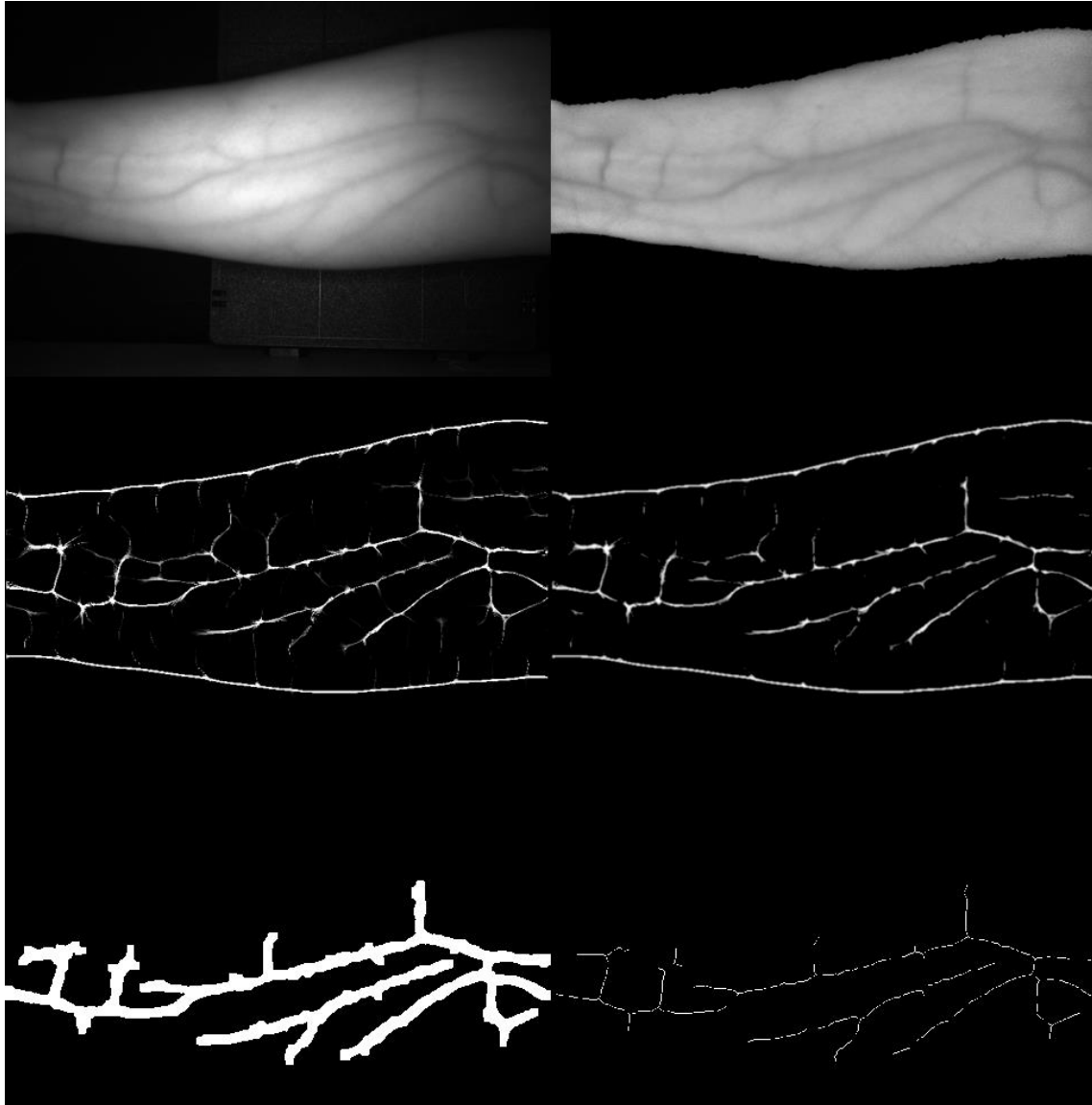
Figure 19 - Segmentation and Skeletonization Steps Visualization.

The top left image is the raw image acquired. The top right image is processed with flat-field illumination correction and local graph cut to remove the background. The middle left image is the result of centerline extraction using maximum curvature methods. The middle right image is a cleanup of the centerlines with below-average and below-median pixels removed. The lower left image is processed with morphological dilation, erosion, connectivity and area filtering, component manipulation. The lower right image is the skeletonization result.

Segmentation and Skeletonization Steps

1) Maximum curvature method with optimized Gaussian filter parameters

2) Remove spurs

3) Repair disjointed path

4) Smooth the centerline

5) Object-based noise removal

6) Skeletonization

1) The maximum curvature method[26] by Miura et al. is used to extract continuous vasculature patterns. The open-source MATLAB vein extraction[27] code is adopted and fine-tuned for my vasculature segmentation. Sigma range from 5-15 is found to be suitable. The algorithm includes three sub-steps to extract vasculature patterns into binarized images.

   a) Extract the vein positions by computing the cross-sectional curvatures of an image, vertically and horizontally and in two oblique directions at 45 degrees, and detects the center of the vasculature at all profiles and evaluates the curvatures with a customized score

   b) Connection of the vein centers by drawing lines to connect the dots

   c) Thresholding the vein pixel values and output a binarized image as the centerline of the vasculature

2) To remove spurs and non-vasculature noise, pixel values below average and below the median are set to zero.

3) To repair disjointed vasculature paths, a few morphological processing techniques are used. Morphological operations such as image erosion, dilation, opening, and closing are

performed and usually using a struct element called strel [28] that is based on the values of the neighborhood.

4) To smooth the vasculature centerline, more morphological operations such as image thinning, area size filter, erosion, dilation, opening and closing are used.

5) Image regions or areas are computed based on connected objects in a binary image. Object areas below two standard deviations are considered noise and removed.

6) Convert binary vasculature image into lines by using morphological skeletonization operation
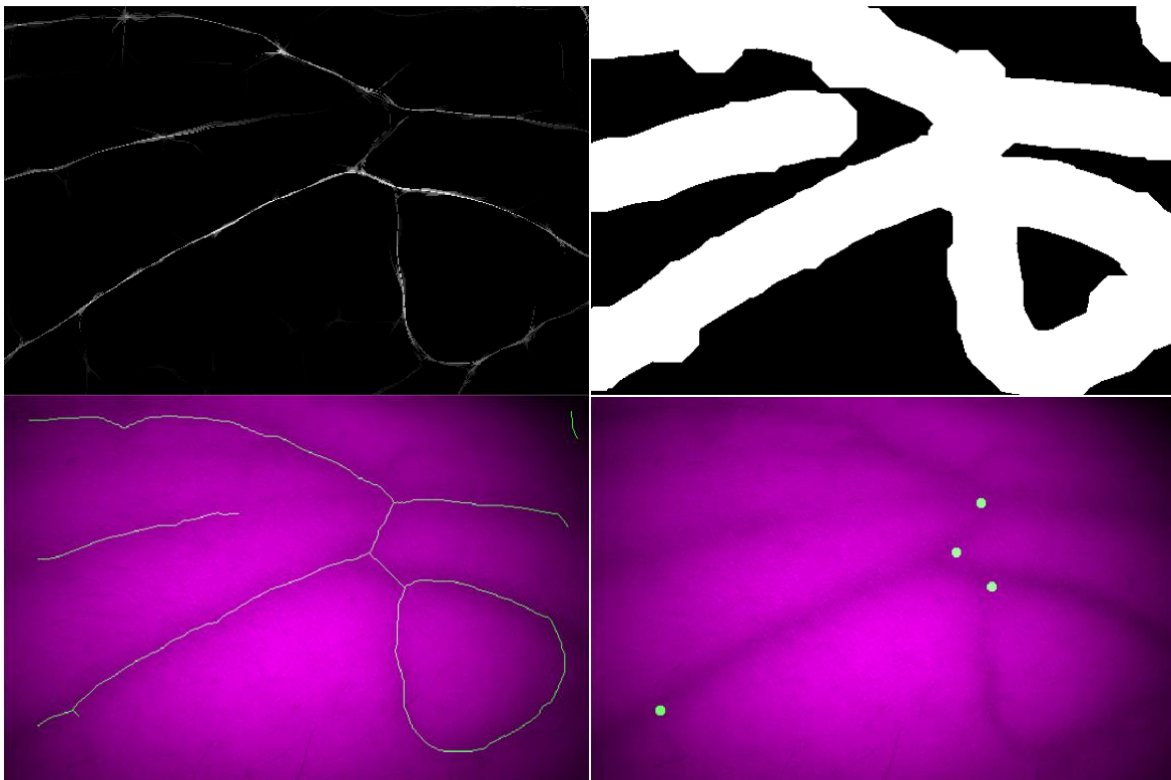
Figure 20 - From Segmentation to Skeletonization to Branchpoint Extraction.

3.2. Registration

Image registration is a technique used to create a homography or stitched image. The technique is used when we want to construct or connect multiple vasculature images into a continuous map. The registration algorithm uses the feature matching functions offered in the Computer Vision Toolbox from MATLAB. The registration results depend on accurate geometric transformations, which are affected by overlapping, prominence, and uniqueness of pixel features.

Registration Steps

1) Load all the images
2) Feature detections between the 'fixed' image and the 'moving image
3) Find matched features and display for visual confirmation
4) Compute geometric transformation (translational and rotational x and y movements) based on image similarity
5) Store and convert local transformations to global coordinates
6) Calculate the panorama size
7) Stitch up all the images based on the array of spatial transformation. Use image warping techniques and the alphablender tool within the computer vision toolbox
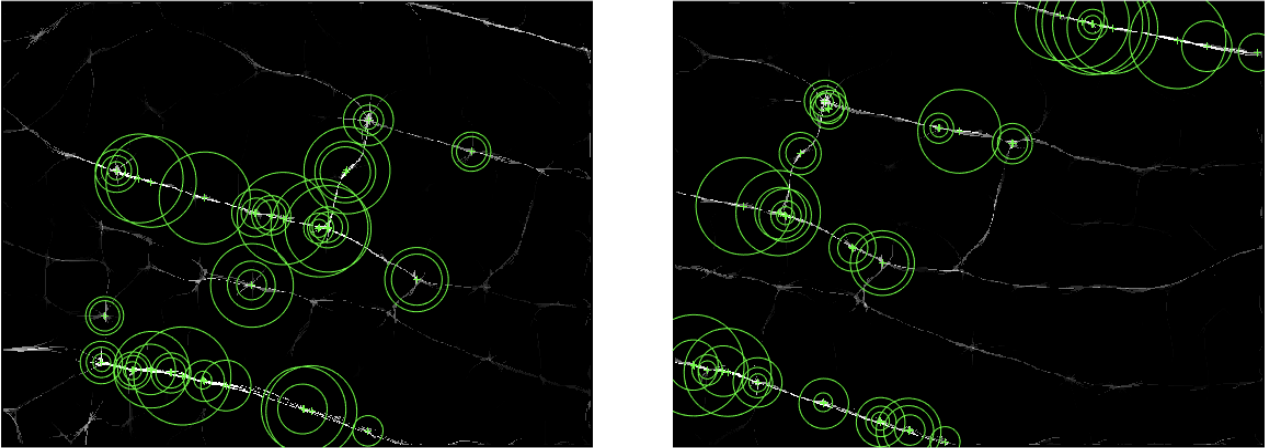
Figure 21 - Feature Detection and Extraction.

The image on the left side is considered as the 'fixed' reference image; the image on the right side as 'moving' image. This figure plots the strongest 50 features detected (described in step 2) from each of the binary images by using the point feature detection algorithm 'detectKAZEFeatures'[29].
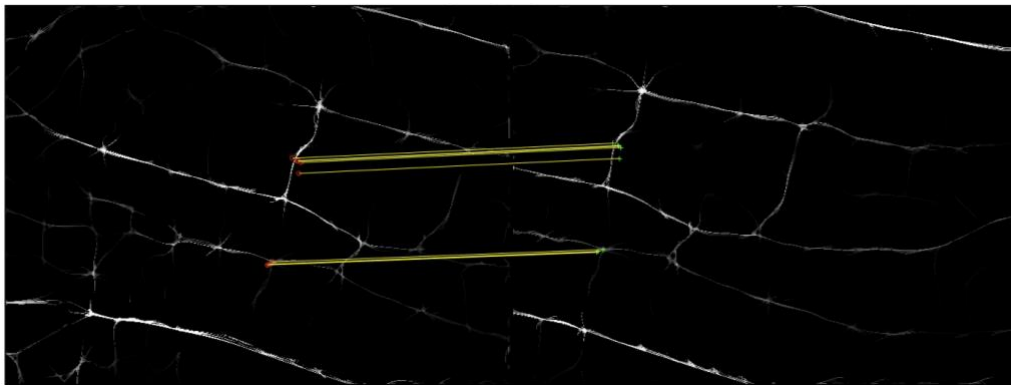
Figure 22 - Feature Matching. This figure displays the matching features results by drawing a yellow line between the matching coordinates from each image in red and green dots.
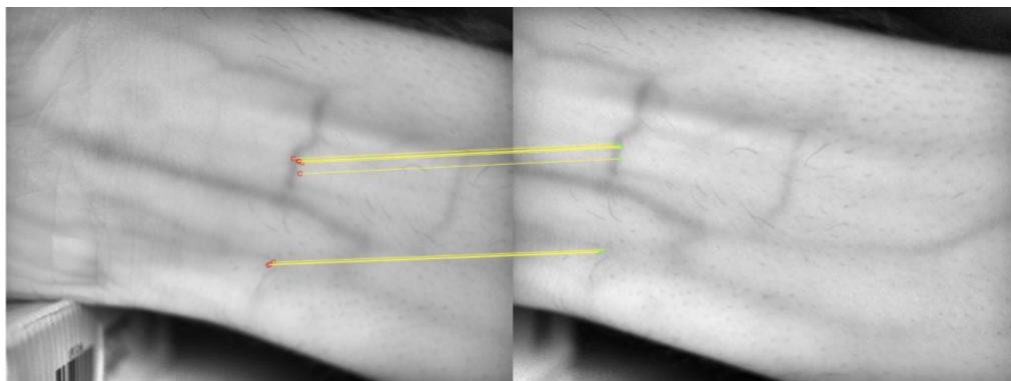
Figure 23 - Feature Matching Overlaid on Raw Images- This plot displays the same matching features results and coordinates overlaid on top of the grayscale images for visual confirmation.
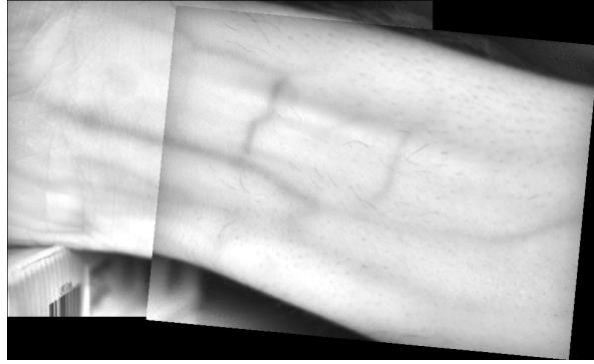
Figure 24 - Registration Result. This figure displays an example of the stitched image using the raw images. While the geometric transformation is stored, the stitching can also be composed with centerline images.

While there are many ways to detect objects and features, the method found with best accuracy is a lightweight point feature detection algorithm called 'detectKAZEFeatures[30]' offered in the MATLAB Computer Vision Toolbox. The decision is driven by a comparison experiment against all other available counterpart point detection algorithms offered. The experiment contains two sets of forearm scans, 6-20 images per scan. To ensure registration accuracy, the geometric matching and transformations have to be linearly consistent. The accuracy score is calculated by visual confirmation of all matched features being parallel and equal distancing.

Feature Detection Algorithms	Accuracy
detectBRISKFeatures	89%
detectFASTFeatures	61%
detectHarrisFeatures	61%
detectMinEigenFeatures	56%
detectMSERFeatures	25%
detectSURFFeatures	99%
detectKAZEFeatures	100%

3.3. Graph-based vasculature network

The graph-based network is a mathematical way (in the sense of graph theory) of representing, processing, and analyzing the relationship between objects. The graph-based method provides a quantitative framework to analyze, store, and reconstruct vasculature networks while maintaining the topological relationship and uniqueness from an individual's vasculature.
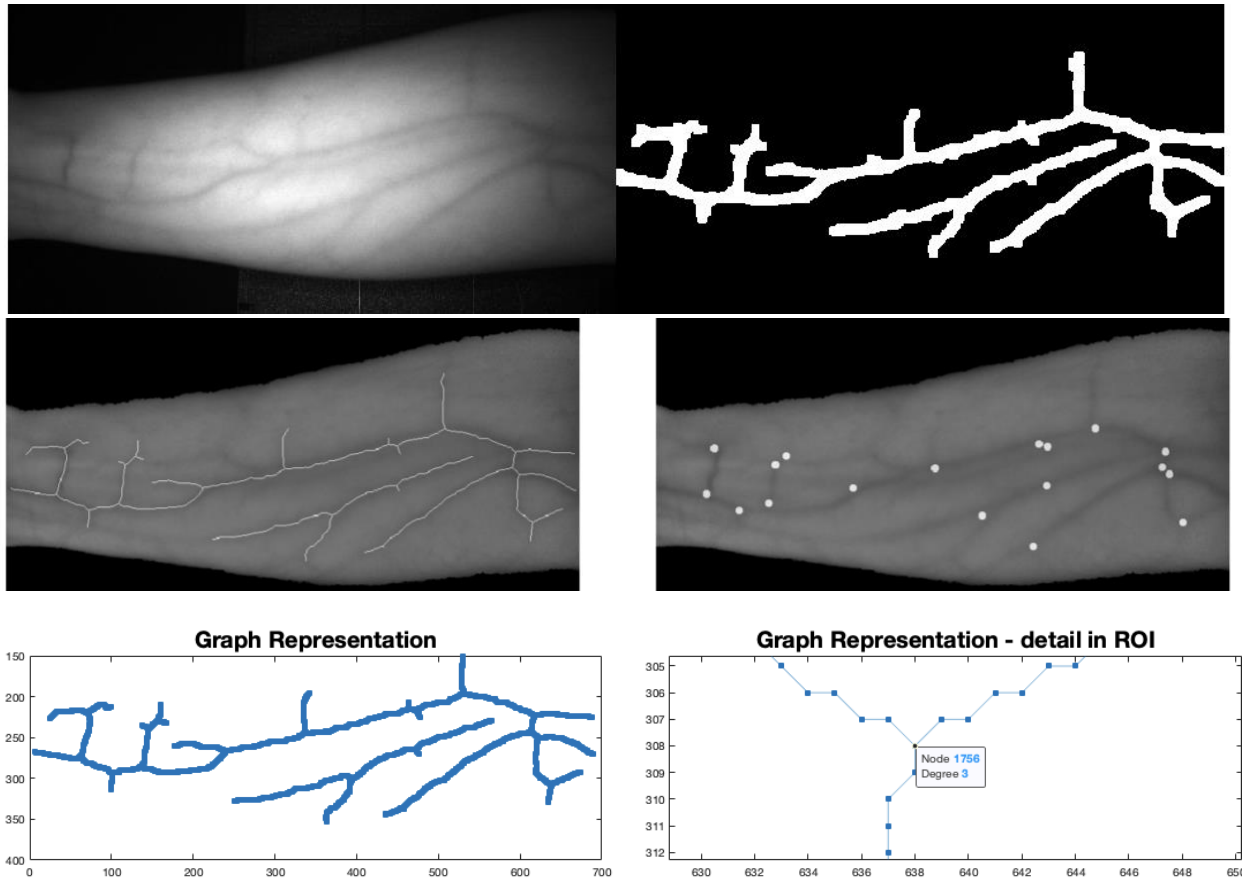
Figure 25 - Overview of Graph-Represented Vasculature Network.

The top left image is from raw image acquisition. The top right image is the result of segmentation and morphological processing to clean up the vasculature geometry. The middle left image is the skeletonization overlaid on the grayscale image. The middle right image shows the branchpoint extracted and displayed as white dots overlaid on the grayscale image. The bottom left plot is the graph-presentation of the vasculature map. The bottom right plot is a zoom-in view of the graph network illustrating a 3 degrees junction point connection.

Steps of converting to graphs

1) Obtain a skeleton of cleanly segmented and binarized vasculature centerline image

2) Convert the skeleton to an unweighted, undirected graph

3) Display edges and nodes by plotting the graph

4) Save and output the graph information. The same graph can be reconstructed by importing and plotting

The example shown above is the graph-representation of a forearm. The characteristics of the graph can be understood by computing the adjacency or incidence matrix. It contains information such as edge-node connection, node-node connection, number of nodes. The junction point is found by computing the degree of freedom of each node. The junction points found in the graph example is 18 and the number of endpoints is 22. The length between any two points can be found by calculating the shortest path; other useful topological information can also be found such as curvature.

There was an attempt to compute the isomorphism between different graphs in order to evaluate the similarity and difference between vasculatures. However, it was determined that graph matching is not applicable given the current processing. Since the current graph conversion method is heavily relying on segmentation, though appropriate semantical vasculature centerlines were segmented, some retaining noise was also carried over to the graph network. An example shown below comes from the same patch of the vasculature, however, the two graph networks are non-isomorphic based on node-edge connections.
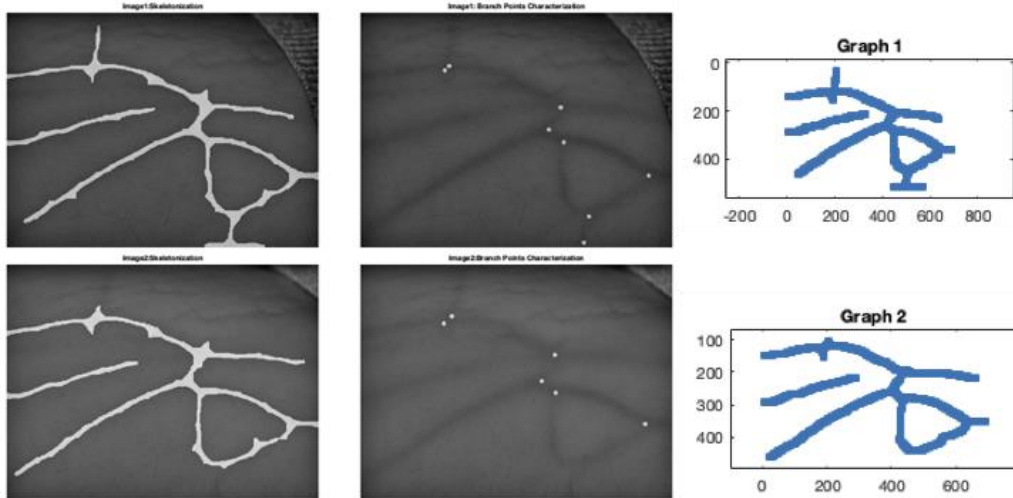
Figure 26 - Graph Comparison between Two Similar Vasculature Networks.

Each row represents data from the same frame. The left column images represent the skeletonization overlaid on the grayscale image. The middle column images represent the brandpoints found overlaid on the grayscale image. The right column images represent the graph-based network conversion.

Graph	Edges	Nodes	# of Junction Nodes (degree>3)	# of End Nodes (degree=1)
Graph 1	2279	2276	16	10
Graph 2	2053	2051	12	8

Despite the unreadiness to use graph-based networks to further perform analysis, the current approach still offers topological insights of the vascular features. It is encouraged for future investigation to overcome the hurdles of suboptimal skeletonization.

3.4. Summary of Methodology

The goal of the imaging processing component is to develop an automated, robust, accurate, and versatile image processing algorithm to enable longitudinal vasculature monitoring. Most of these goals have been achieved by developing a clean method for segmentation and skeletonization, expanding the homography to both binary images and grayscale raw images, and through preliminary work on the graph-represented method. These improvements hopefully help with future studies of vasculature networks.

Additionally, it is also important to discuss and document the limitations of the current methodologies. In some instances where two images failed to be registered or relocalized, one of the reasons could be due to large angular rotation which caused unmatched features from different viewing angles. This unwanted rotation is likely introduced by free-hand operations and can be addressed by designing and building some fixtures to limit the amount of movement. Another possibility can be due to the disjoint path from an individual's anatomical structure, which is likely caused by depth variation but does not refer to disjoint vasculature. Currently, the algorithm purely relies on the saliency of vascular features. Potential solutions can include adopting another location reference system, such as IMU sensor, or adopting 3D stereo imaging techniques. Also described in section 5.2, future work may include more investigation on centerline repairing/cleaning algorithms, such as centerline shifting algorithms, to fix disjoint paths.

4. Results

This chapter presents some vasculature analysis results to demonstrate the device's robustness and computation capabilities. Three major types of studies have been performed: (1) longitudinal vasculature stability comparison, (2) individual vasculature uniqueness and registerability, and (3) exploration of vascular visibility on different human body locations.

4.1. Longitudinal Vasculature Data

Superficial vasculature on the human body is a relatively stable network (section 1.4) while it is possible for adults to form neovascularization, the literature indicates that angiogenesis under non-stimulated conditions is generally associated with pathophysiological conditions[31] such as tumorigenesis, ischemic insult, and chronic inflammatory diseases.

Same subject vasculature homography (data from 2017)
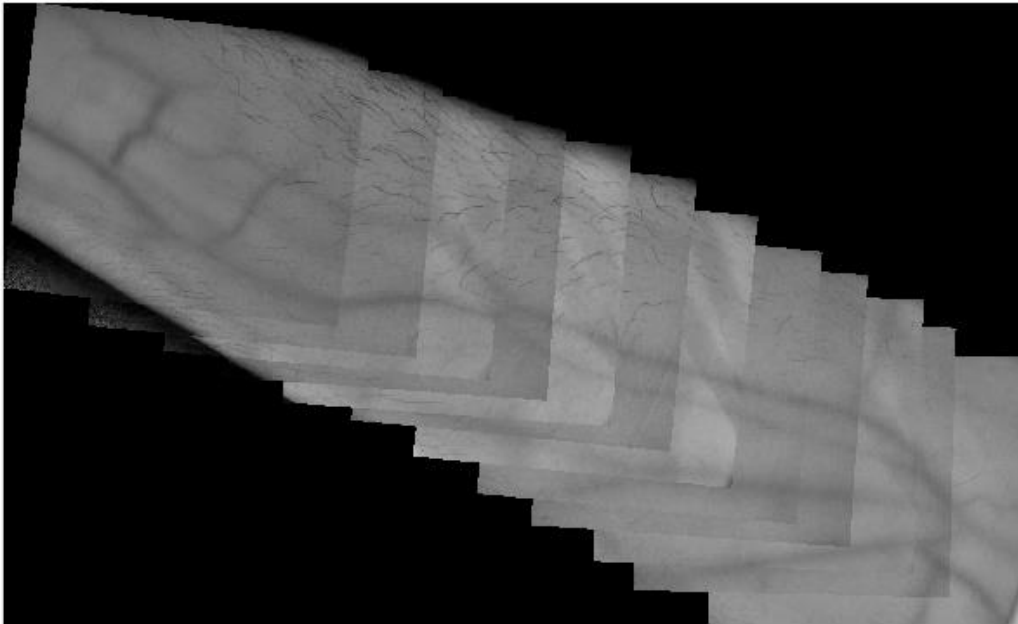
Figure 27 - A Stitched Vascular Map of A Forearm with Data from 2017 from the same subject.

A homography is recently created using the registration algorithm developed for the thesis, and the raw images were acquired in 2017.

Same subject vasculature homography (data from 2020)
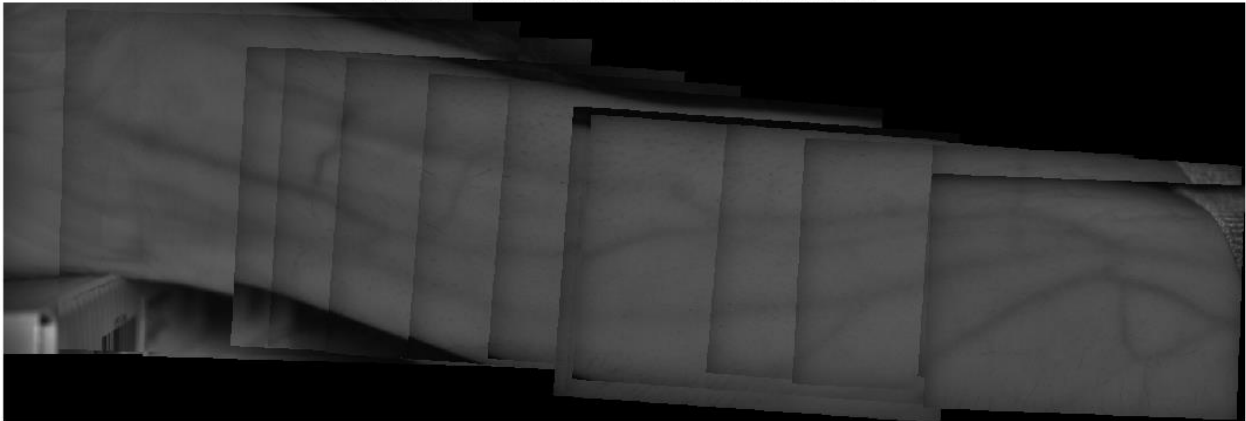
Figure 28 - A Stitched Vascular Map of A Forearm with Data from 2020 from the same subject.

A homography is created using the registration algorithm developed for the thesis, and the raw images were acquired in 2020.

In the interest of investigating vasculature stability on adults, we are interested in collecting data across different time spans. From previous research (section 1.5)[5], vascular data were compared across an eight-month time span. To provide some more evidence of a stabilized

longitudinal vasculature network, the vasculature images on a healthy volunteer's forearm between 2017 and 2020 are acquired, stitched, and displayed in figure 27 and figure 28. From a qualitative approach with human eye confirmation, the vasculature homography between 2017 and 2020 looks unique and recognizable as the same network; the blood vessel sizing, branches, and geometry relationship also look very comparable. Between the two stitched vascular maps, no new vasculature is observed. Even though some blood vessel branches appear in lower contrast, it is most likely due to imaging conditions, camera settings, or forearm positioning.

4.2.   Relocalization

Considering the overarching goal of the system is to monitor superficial vasculature longitudinally, being able to register and re-localize is an important task and provides tremendous values to monitor any vascular changes. Relocalization in computer vision refers to the capability of registering any frame to a pre-existing scene, which is a vasculature map in our application. Relocalization capability allows for immediate visual comparison, side-by-side or overlay, as well as any further topological analysis.

Two methods were adopted for vasculature relocalization: direct image matching[32] and feature-based mapping. For direct image matching method, the images are processed with Gaussian blurs to enhance intensities and pixel structures. For feature-based mapping, the images can either be Gaussian blurred images or with centerline extraction (section 3.2) where the comparison happens between the chosen descriptors (SURF[33], KAZE[30]). Two methods were both illustrated below.
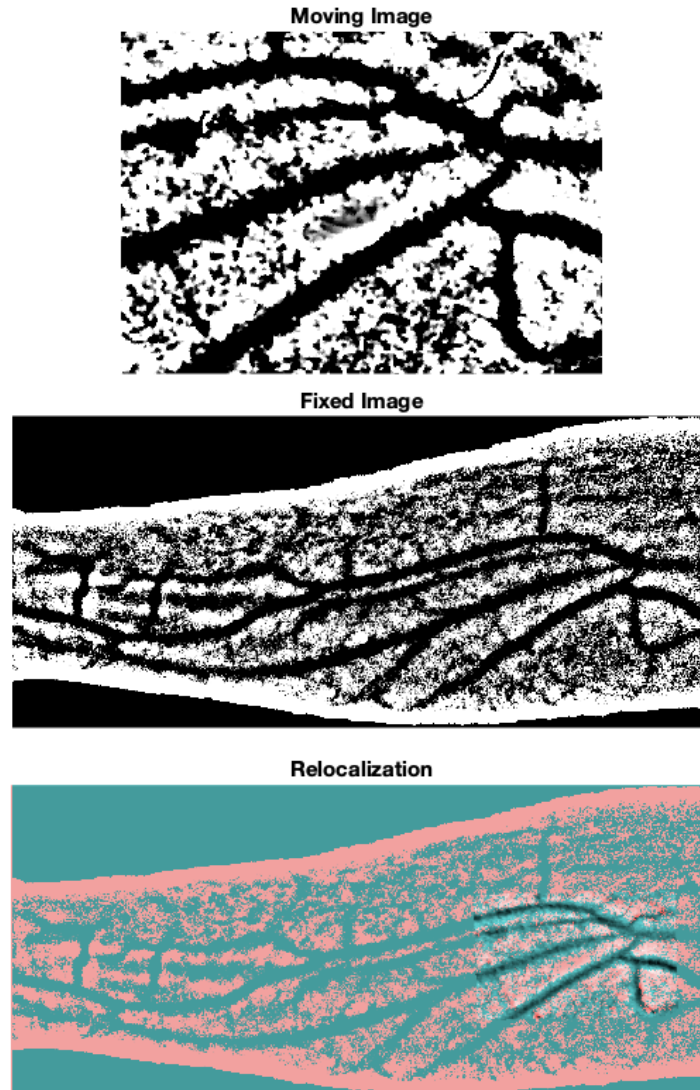
Figure 29 - Relocalization Overview.

This figure presents forearm data across a two-year span. From top to bottom, 'Moving image' is a small patch of vasculature collected in 2018. 'Fixed image' is a vasculature map of a forearm collected in 2020 from the same subject. 'Relocalization' is the registered result with the transformed 'moving image' overlaying on top of the 'fixed image'. In the 'relocalization' image, red and cyan color each represents an output channel, red indicates the original white pixels from the 'fixed image', cyan indicates the original white pixels from the 'fixed image', white indicates the pixel difference between the 'fixed image' and the transformed 'moving image', black highlights the similarity between the two.

The relocalization data in figure 25 represents forearm data from two years apart from the same healthy volunteer. The 'Moving Image' was acquired in 2018 and processed with Gaussian blur filter; the 'Fixed Image' was a map of the full forearm acquired in 2020, and the same Gaussian blur filter treatment. The transformation is computed using the affine geometric transformation method [34] and the gradient descent optimization[35] algorithm, such that the

direction of gradient change was calculated, and the mean square error of the pixel difference was minimized to find matches between two images. The gradient descent optimization method can be used on images with varying intensity, and is great for images with similar brightness and contrast, but not very useful on the centerline extraction images. Another important factor is to have a good initial guess in order to best achieve searching results and reduce steps. Hence, an intermediate measure is taken before the gradient descent registration method. Two-dimensional cross-correlation [36] analysis is performed on both the moving and fixed images to provide an initial, approximate geometrical fitting within the entire vasculature map, the output maxima indexes is then used to find the approximate fitting. In signal processing, cross-correlation is commonly known to find the regions in which two signals most resemble each other; in this application, due to the stability and uniqueness of vascular features, it is also useful in the vasculature relocalization process.

For feature-based relocalization, it is very sensitive to illumination changes and noise pixels over different frames could change the appearance of the point features substantially. Hence feature-based relocalization is great for the same scanning relocalization and registration (section 3.2), especially centerline extracted images under the same illumination conditions.

4.3.   Visibility of Vasculature from Different Locations

The visibility of superficial vasculature not only varies across different individuals and skin tones (section 1.3) but also varies based on body locations. Scans are collected from different body locations, including chest, forearm, abdomen, lower and upper legs, to compare the vasculature visibility and vascular features.

The vasculature exploration is performed on a few volunteers. Even though some scans were not captured due to insufficient vasculatures, the following table contains empirical observations from different areas based on visibility and image quality (for segmentation and

46

processing purposes). Some physiological factors are related to the blood vessel visibility including the proximity to the skin surface, features uniqueness and geometry (straight line vs. loop), level of vascular prominence, and sizing. Other tangible elements that affect the raw image qualities are non-uniform surfaces and curvatures on different parts of the body. This presents unwanted edges and features mixed with the vasculature, as well as creates non-uniform light distribution and shades.

Body Location	Vasculature Visibility	Image Quality
Forearm	✓✓	✓✓
Chest	✓✓✓	✓✓✓
Lower abdomen	✓✓	✓
Upper abdomen	x	
Lower Leg	✓	x
Upper Leg	✓✓✓	✓
Hand & foot	✓✓	x
Back	x	
Neck	x	
Face	x	
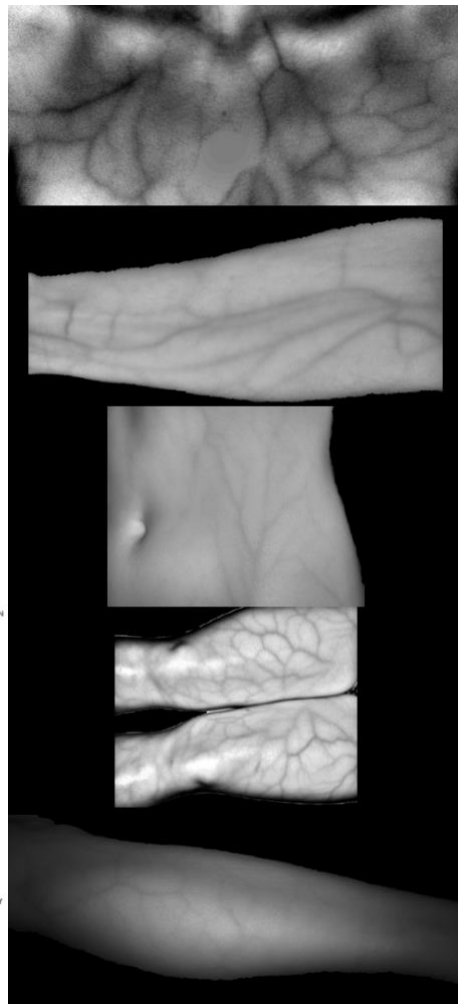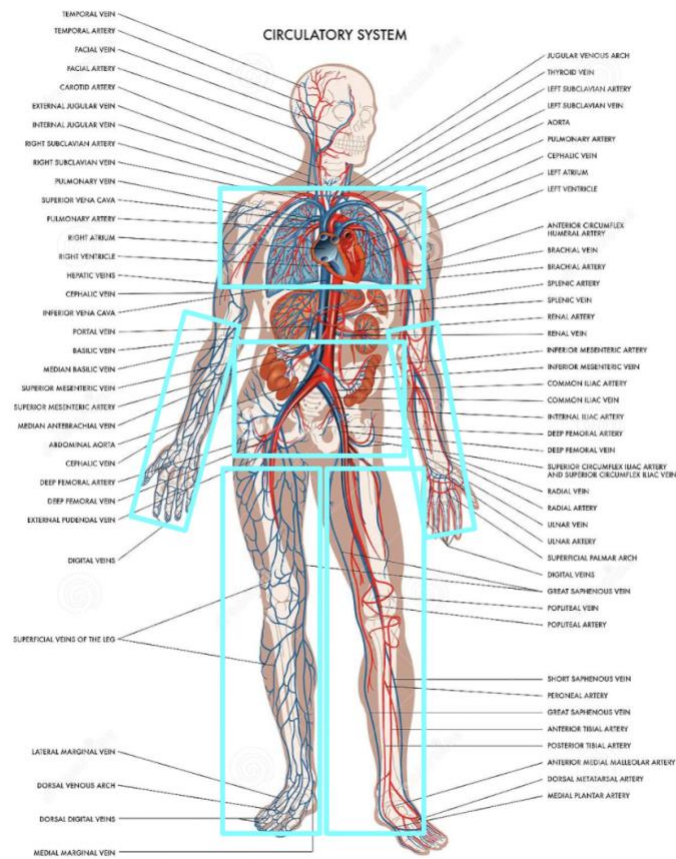
Figure 30 - (on the left side) This figure displays vasculature data acquired at different body locations. From top to bottom, the locations are chest, forearm, abdomen, upper leg, lower leg.

Figure 31 - (on the left side) This figure shows the locations where data were collected for vasculature visibility exploration.
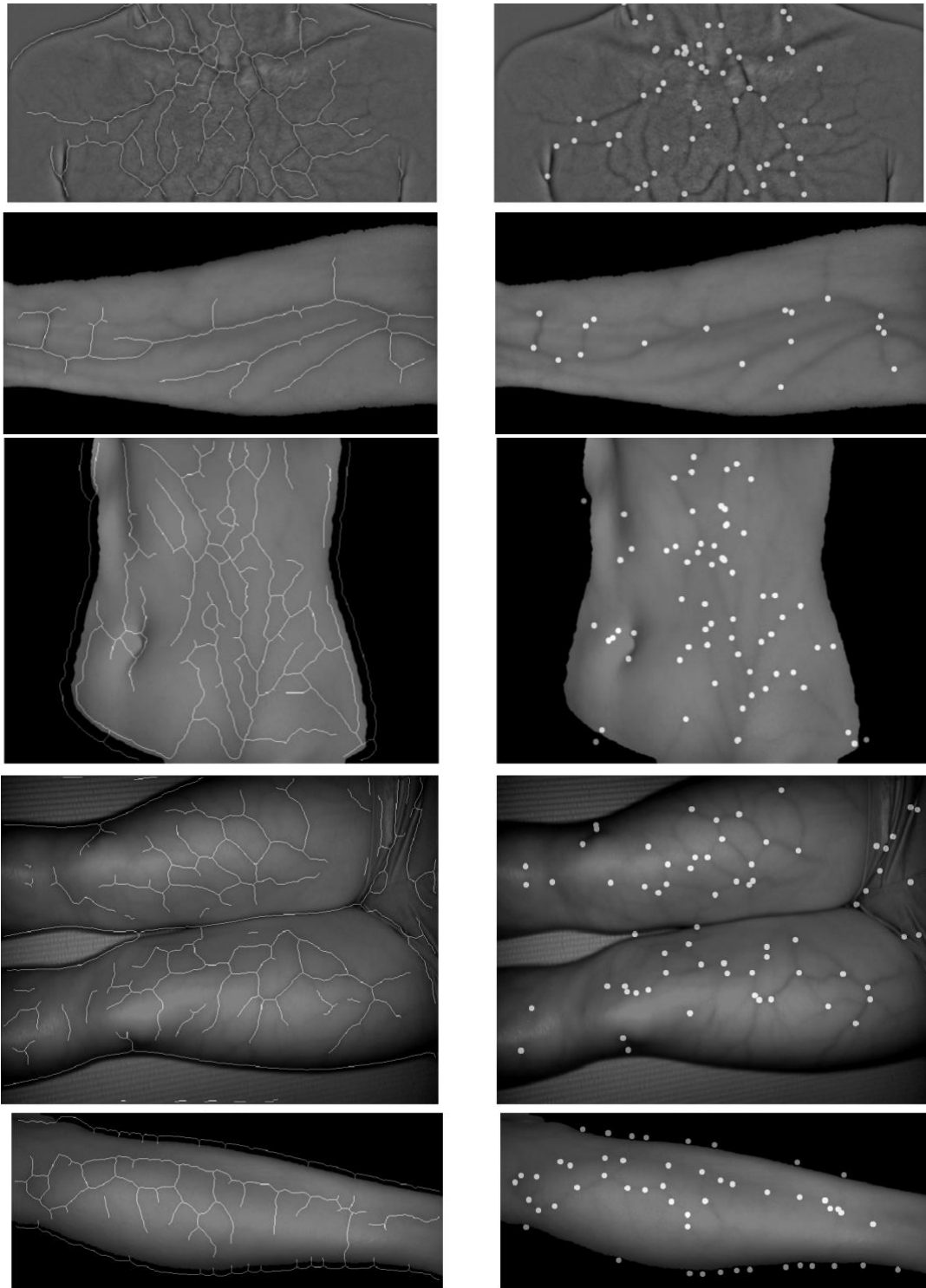
Figure 32 - Comparison of Vasculature Visibility from Different Body Locations.

This figure displays vasculature analysis at different body locations (from top to bottom, the locations are chest, forearm, abdomen, upper leg, lower leg). The left column images show the skeletons (displayed in white lines) overlaid on the grayscale image, the right column images show the found branchpoints/ junction nodes (displayed in white dots).

The table below summarizes the vascular features into the number of junction nodes and end nodes from the skeleton's information above representing different body locations. Overall a higher number of junction nodes correlates with a higher level of vasculature uniqueness (since the junction points represent unique features such as bifurcation or loops); the number junction nodes do not correlate with the amount of vasculature.

Graph	# of Junction Nodes (degree>3)	# of End Nodes (degree=1)
Chest	67	55
Abdomen	66	48
Lower Leg	51	49
Upper Leg	70	114
Forearm	18	22

The comparison and capturing of vasculature across different locations of the body can provide a better understanding and reference for future subcutaneous vasculature studies, regardless of clinical or non-clinical applications. Another observation is that, even though there are variations (vasculature visibility, diameter, contrast, and connectivity) between different individuals, these elements are noticed consistently within the same person.

4.4.   Summary of Vasculature Analysis Results

Considering the clinical and non-clinical applications of NIR vasculature imaging, it is of interest to test and analyze the capability of longitudinal angiogenesis monitoring and relocalization. Under an MIT IRB protocol, 5 human subjects were studied, and a number of 15 scans were acquired from 5 different locations of the body. We also have some prior collected data from our research lab, in which two sets of data were acquired from the same subjects volunteered in recent studies. All scans were successfully analyzed, segmented, stitched, skeletonized, graph-converted, re-localized. The developed algorithms and processes are

considered quite robust for computing the relative changes or differences between longitudinal vasculature.

The exploration of subcutaneous vascular visibility has offered new insights for future NIR vascular imaging work. Current information regarding vasculature diameter, contrast, connectivity, and shapes is observational and qualitative. To better understand the correlations and variants, a larger sample size should be investigated, and more metrics should be defined and used to make quantitative measurements.

5.   Conclusion

The technology of NIR imaging of the subcutaneous vasculature has the potential in many clinical and scientific applications. By studying the vascular network longitudinally, a broader picture of vascular disease progression and manifestation can provide more health information in a non-invasive manner. The stability and uniqueness of a vascular network not only provide a reference platform to measure any vascular changes, but can also be used for biomarkers such as a personal identifier or a relocalization tool. To better enable studies about superficial vasculature, my thesis work is on the development of both the tangible system and computational framework to support information extraction from the vascular networks. This chapter presents some of my learnings and discussion about future work.

5.1.   Learnings

The development progress has been iterative and reflective. One of the biggest realizations learned is the intercorrelated efforts between hardware development and algorithm development. To achieve consistent results, consistent optical settings (working distance, exposure, ROI) and conditions (illumination intensity and distribution) are key. However, we would

also like to keep the NIR imaging device versatile and highly customizable, for wide adaptation to different studies (different parts of human bodies, different skin tones, and imagery environments). Hence for future recommendations, more work shall be put into designing and developing a versatile mechanical reference system. The requirements would be the direct measurement from imagery surface, adjustable length, linearly movement, modular, and easy to change settings and use.

5.2.   Future Work

5.2.1.   Future Optics

Some recommendations on future optics exploration. The current Manta camera is the state-of-the-art NIR camera that is commercially available. Even then, the quantum efficiency percent at imaging wavelength 880nm is still no more than 25%, as shown below.
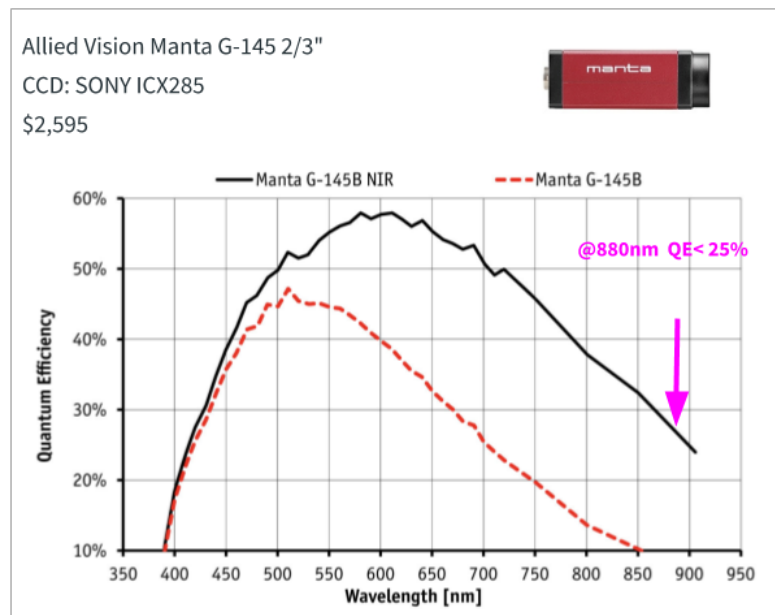
Figure 33 - Quantum Efficiency of Manta G-145 NIR camera at 880nm
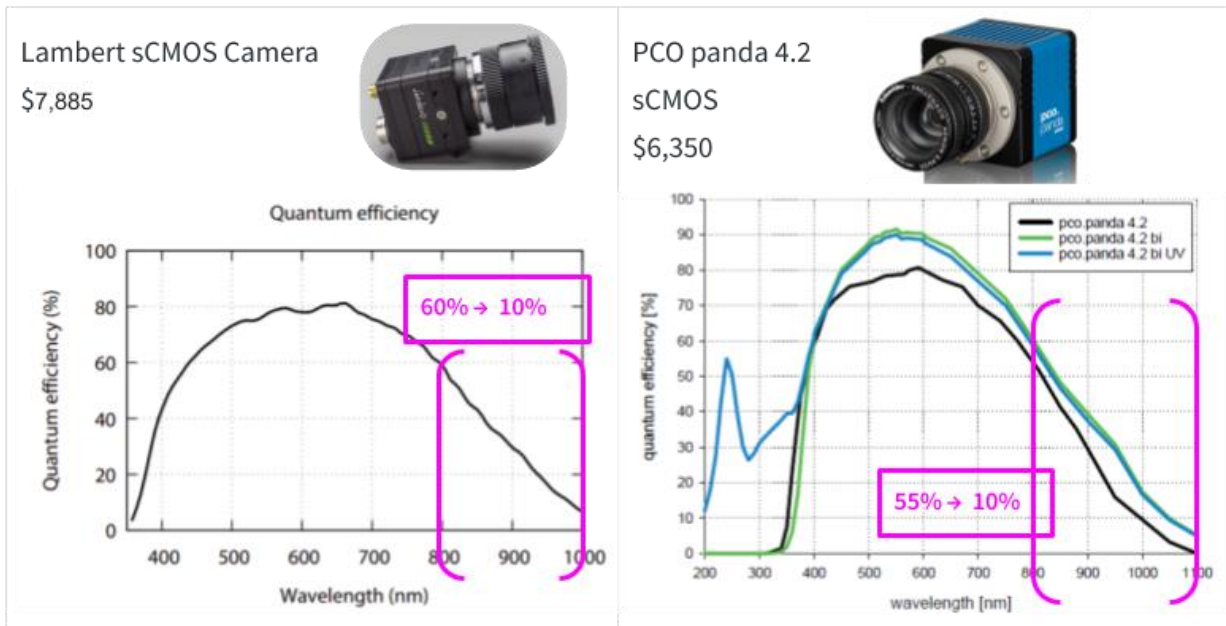
Figure 34 - Quantum Efficiency of sCMOS sensors in the NIR range

The sCMOS sensor (stands for scientific CMOS), shows better sensitivity in the NIR range. This type of scientific camera[37] is designed for microscope purposes with high dynamic range and low read noise. By using a scientific sCMOS camera in conjunction with a NIR specified polarized filter, this should significantly improve the consistency and raw image quality, in terms of vascular contrast to other tissues. Using the scientific type of camera might be able to pick up smaller blood vessels that normally cannot be differentiated.

Multi-spectral imaging is another suitable technology for human tissue imaging. Multi-spectral camera works by capturing image data with specific wavelengths[38], and usually the image data is filtered at each specific wavelength. Most of the multispectral camera is customized designed for high-end applications, such as military tracking; hence highly customized spectral bands and the number of bands can be chosen to optimize for the application. Similarly to an RGB camera, the data output contains three-channel information, but differently from an RGB camera, multi-spectral camera outputs spectral imaging information in 3-dimensional as a data cube. By leveraging the absorption coefficient for different types of tissues, the multi-spectral

imaging would certainly be a significant upgrade to study superficial vasculature. Using multi-spectral imaging, it is also hopeful that the oxygenation level and perfusion can be recorded. Holmer et al[39] have performed a controlled study in 2016 by using a multispectral camera to extract oxygen saturation level (SO_2) from non-contact hand imageries.
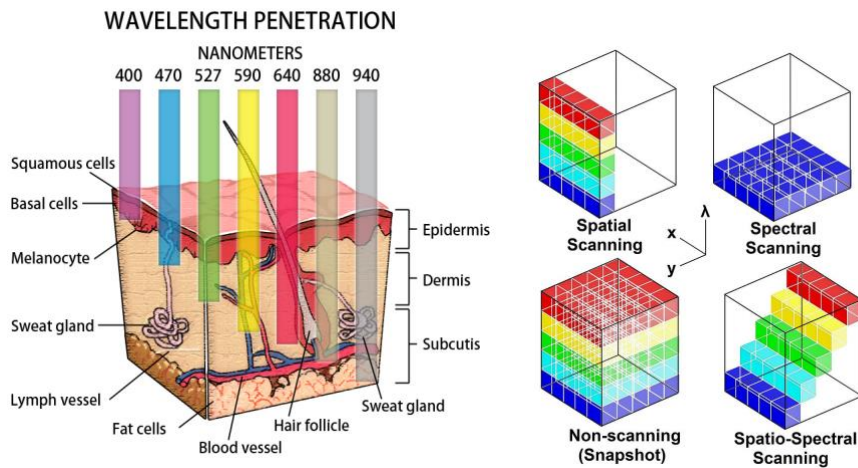
Figure 35 - (right) 3D Data Cube Representing Data Output from Multi- Spectral Imaging

Figure 36 - (left) Simplified Illustration of Wavelength Penetration of the Skin.

If multispectral imaging is used, the research goal can be expanded and/or pivoted to a broader range of topics such as vascular circulatory information. An interesting use case would be to non-invasively gather oxygenation data without contact during the COVID-19 pandemic situation.

5.2.2. Future Illumination

The current illumination source is a NIR LED light ring at 880nm (section 2.2) and it is chosen to highlight hemoglobin absorption. A detailed look at the molar extinction spectrum from figure 6 (log scale) reveals the absorption between hemoglobin and deoxygenated hemoglobin is different at different wavelengths, and the total effective absorption is also different. For future work, it would be interesting to explore the difference between the two. As mentioned above, one

way to do this is to use a multi-spectral camera. another way could be using a multi-spectral light source with wavelength-specific filters.

There was an attempt to create multi-wavelength custom LEDs (850nm, 940nm) as shown in figure 38 below. However the non-uniform and narrow-angle light distribution presented challenges during the experiments. For future proof-of-concept, the recommended approach would be to purchase a multi-channel NIR light source, where it is most commercially available amongst night-mode security light sources, as well as wavelength-specific filters.
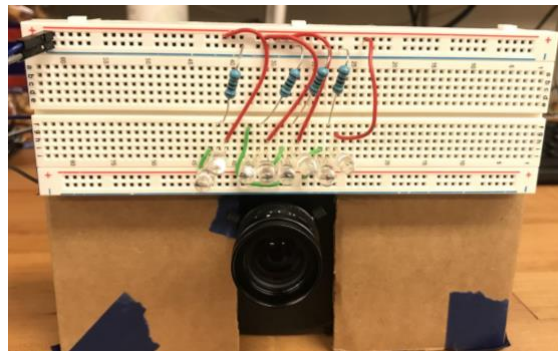
Figure 37 - Prototype of a Custom Wavelength LED lights.

5.2.3. Future Validation

The current system and algorithm are capable of stitching vascular maps using feature-detection algorithms. Through visual confirmation, all vein maps were appropriately stitched. For longitudinal vascular monitoring, even though it is important to monitor new changes, it also seems that comparing the vasculature to the ground truth would be beneficial to further characterize the imaging system. Also, to address instances where the path appears disjointed due to the individual's physio-anatomical difference in vasculature near-surface level and size, shape, having a validation method to compare the results to ground truth would be an appropriate future step for this project.

Approaches for additional validation systems include: (1) external camera-positioning measurement (IMU sensor, camera motion tracking such as OptiTrack) (2) additional imaging modalities (Angiogram, CT, ultrasound), and (3) 3D stereo NIR camera for spatial mapping .

5.2.4.   Future Applications

NIR vasculature imaging technology can have many other potential applications. For example, biometric identifiers for smartwatches, venous disease progression monitoring, non-contact oxygenation level measurement.

For smartwatches like Apple Watch, the wearable is attached to the wrist, where radial and ulnar arteries and veins vasculature are available and salient. It would be beneficial to take advantage of the uniqueness of vasculature and use the vasculature information as a personal identifier. This would be an easy and natural way to unlock the wearable device without additional effort. The challenges in this application might be the form factor and further quantification method to process and store the vascular features. The form factor of the imaging sensor can also be alternatively minimized to lensless imaging.

The essence of the system is to monitor any longitudinal changes and achieve localization and topological analysis. This system can be a useful tool for any venous disease (varicose vein, superficial thrombophlebitis), and venous-manifest symptoms. For example, a recent hypothesis for COVID-19 symptoms with rashes on the skin[40] and frostbite-like coloration on the fingers and toes (also widely known as COVID toes) is that these symptoms might be associated with deep-vein thrombosis; no answers have been revealed yet. If these symptoms were potentially associated with hemoglobin level changes, it could be monitored using the NIR imaging system.

Non-contact oxygenation level measurement would be an exciting and compelling research goal for the next step. Unfortunately, due to the COVID-19 pandemic, the demands for non-contact health surveillance have significantly increased to ensure the health and safety of our communities. The NIR imaging device, as discussed in the future camera section 5.2.1,

leveraging the wavelength-specific data with multi-spectral imaging could potentially enable the capability of non-contact oxygenation level or perfusion measurement.

5.2.5. Future Image Processing and Analysis

To better study vasculatures, it is encouraged to improve segmentation and relocalization performance. For relocalization purposes, the current imagery in 2D has registration limitations if without external location reference. If the vasculature data is captured with 3D stereo NIR camera[41], the blood vessels shall be extracted into 3D point clouds with more inclusive data points available and improve the registration performance.

To further bridge the gap between research and application, there shall be more standard metrics and parameters to quantify the vascular patterns, features, and physiological relationship (depth & location of vasculature). Accurate vasculature analysis and registration demand a clean level of segmentation and topological processing. Methods to improve segmentation may include centerline cleaning and repair algorithms, such as the centerline shifting method[42] and Gaussian curvature[43] for smooth medial axis cleaning[44]. Methods for graph network topological analysis may include node-to-node analysis (shortest path, nearest neighbors, curvature, connectivity, etc.) and node-to-cluster analysis (transitivity, Euler characteristic, areas, classification, etc.)[45].

List of Reference

[1] "Vascular Diseases, Arterial Disease and Venous Disease," *Minimally Invasive Vascular*. https://mivascular.com/vascular-diseases/ (accessed Apr. 15, 2020).

[2] "Varicose veins - Symptoms and causes," *Mayo Clinic*. https://www.mayoclinic.org/diseases-conditions/varicose-veins/symptoms-causes/syc-20350643 (accessed May 14, 2020).

[3] "Slideshow: Spider and Varicose Veins: What Causes Them? What Can You Do?," *WebMD*. https://www.webmd.com/skin-problems-and-treatments/ss/slideshow-spider-varicose-veins (accessed May 14, 2020).

[4] L. Rey-Barroso *et al.*, "Visible and Extended Near-Infrared Multispectral Imaging for Skin Cancer Diagnosis," *Sensors*, vol. 18, no. 5, May 2018, doi: 10.3390/s18051441.

[5] K. Benjamin and I. Annesha, "Imaging skin structures for health, body mapping, and identification (under the Tucson Skin)," Thesis, Massachusetts Institute of Technology, 2018.

[6] K.-A. Toh and A. B. J. Teoh, "Vascular Patterns," in *Encyclopedia of Cryptography and Security*, H. C. A. van Tilborg and S. Jajodia, Eds. Boston, MA: Springer US, 2011, pp. 1353–1356.

[7] P. Tower, "The Fundus Oculi in Monozygotic Twins: Report of Six Pairs of Identical Twins," *AMA Arch. Ophthalmol.*, vol. 54, no. 2, pp. 225–239, Aug. 1955, doi: 10.1001/archopht.1955.00930020231010.

[8] A. Jain, A. Ross, and S. Prabhakar, "Fingerprint matching using minutiae and texture features," in *Proceedings 2001 International Conference on Image Processing (Cat. No.01CH37205)*, Oct. 2001, vol. 3, pp. 282–285 vol.3, doi: 10.1109/ICIP.2001.958106.

[9] H. C. A. van Tilborg and S. Jajodia, Eds., *Encyclopedia of Cryptography and Security*. Boston, MA: Springer US, 2011.

[10] A. I. Chen, M. L. Balter, T. J. Maguire, and M. L. Yarmush, "3D Near Infrared and Ultrasound Imaging of Peripheral Blood Vessels for Real-Time Localization and Needle Guidance," in *Medical Image Computing and Computer-Assisted Intervention - MICCAI 2016*, Cham, 2016, pp. 388–396, doi: 10.1007/978-3-319-46726-9_45.

[11] T. Van Tien, P. T. H. Mien, P. T. Dung, and H. Q. Linh, "Using Near-Infrared Technique for Vein Imaging," in *5th International Conference on Biomedical Engineering in Vietnam*, Cham, 2015, pp. 190–193, doi: 10.1007/978-3-319-11776-8_46.

[12] N. J. Cuper *et al.*, "The use of near-infrared light for safe and effective visualization of subsurface blood vessels to facilitate blood withdrawal in children," *Med. Eng. Phys.*, vol. 35, no. 4, pp. 433–440, Apr. 2013, doi: 10.1016/j.medengphy.2012.06.007.

[13] "VeinViewer Vision2," *Christie Medical Holdings*. https://christiemed.com/products/vienviewer-models/veinviewer-vision2/ (accessed May 15, 2020).

[14] "Veinsite®," *VueTek Scientific*. https://vuetekscientific.com/veinsite-vein-finder/ (accessed May 15, 2020).

[15] A. M. Smith, M. C. Mancini, and S. Nie, "Second window for in vivo imaging," *Nat. Nanotechnol.*, vol. 4, no. 11, pp. 710–711, Nov. 2009, doi: 10.1038/nnano.2009.326.

[16] S. L. Jacques, "Optical properties of biological tissues: a review," *Phys. Med. Biol.*, vol. 58, no. 11, pp. R37–R61, May 2013, doi: 10.1088/0031-9155/58/11/R37.

[17] "Near-infrared window in biological tissue," *Wikipedia*. Mar. 31, 2020, Accessed: Apr. 20, 2020. [Online]. Available: https://en.wikipedia.org/w/index.php?title=Near-infrared_window_in_biological_tissue&oldid=948386540.

[18] PDQ Screening and Prevention Editorial Board, "Skin Cancer Prevention (PDQ®): Patient

Version," in *PDQ Cancer Information Summaries*, Bethesda (MD): National Cancer Institute (US), 2002.

[19] "Layers of the Skin - Anatomy and Physiology - OpenStax." https://openstax.org/books/anatomy-and-physiology/pages/5-1-layers-of-the-skin (accessed Apr. 20, 2020).

[20] "Ch. 1 Introduction - Anatomy and Physiology | OpenStax." https://openstax.org/books/anatomy-and-physiology/pages/1-introduction (accessed May 13, 2020).

[21] B. AG, "Basler ace acA2000-165um - Area Scan Camera," *Basler AG*. /en/products/cameras/area-scan-cameras/ace/aca2000-165um/ (accessed May 13, 2020).

[22] "Allied Vision Manta G-145 NIR Camera | Edmund Optics." /p/allied-vision-manta-g-145-23-nir-ccd-camera/29709/ (accessed May 13, 2020).

[23] "Allied Vision Mako G-419B Camera | Edmund Optics." /p/allied-vision-mako-g-419b-1-nir-cmos-camera/30730/ (accessed May 13, 2020).

[24] "2-D image flat-field correction - MATLAB imflatfield." https://www.mathworks.com/help/images/ref/imflatfield.html (accessed May 14, 2020).

[25] "Segment Image Using Local Graph Cut (Grabcut) in Image Segmenter - MATLAB & Simulink." https://www.mathworks.com/help/images/segment-image-using-local-graph-cut-grab-cut.html?s_tid=srchtitle (accessed May 08, 2020).

[26] N. Miura, A. Nagasaka, and T. Miyatake, "Extraction of Finger-Vein Patterns Using Maximum Curvature Points in Image Profiles," *IEICE Trans. Inf. Syst.*, vol. E90-D, no. 8, pp. 1185–1194, Aug. 2007, doi: 10.1093/ietisy/e90-d.8.1185.

[27] "Miura et al. vein extraction methods." https://www.mathworks.com/matlabcentral/fileexchange/35716-miura-et-al-vein-extraction-methods (accessed May 08, 2020).

[28] "Morphological structuring element - MATLAB." https://www.mathworks.com/help/images/ref/strel.html (accessed May 08, 2020).

[29] "Object Detection Using Features - MATLAB & Simulink." https://www.mathworks.com/help/vision/object-detection-using-features.html?s_tid=CRUX_lftnav (accessed May 09, 2020).

[30] "Detect KAZE features - MATLAB detectKAZEFeatures." https://www.mathworks.com/help/vision/ref/detectkazefeatures.html (accessed May 12, 2020).

[31] R. K. Bruick and S. L. McKnight, "Building better vasculature," *Genes Dev.*, vol. 15, no. 19, pp. 2497–2502, Oct. 2001, doi: 10.1101/gad.931601.

[32] "Image-based Relocalization in SLAM - Yu Huang's webpage." https://sites.google.com/site/yorkyuhuang/home/research/computer-vision-augmented-reality/image-based-relocalization-in-slam (accessed May 12, 2020).

[33] H. Bay, T. Tuytelaars, and L. Van Gool, "SURF: Speeded Up Robust Features," in *Computer Vision – ECCV 2006*, vol. 3951, A. Leonardis, H. Bischof, and A. Pinz, Eds. Berlin, Heidelberg: Springer Berlin Heidelberg, 2006, pp. 404–417.

[34] "Affine Transformation." https://www.mathworks.com/discovery/affine-transformation.html (accessed May 12, 2020).

[35] "Regular step gradient descent optimizer configuration - MATLAB." https://www.mathworks.com/help/images/ref/registration.optimizer.regularstepgradientdescent.html (accessed May 12, 2020).

[36] "2-D cross-correlation - MATLAB xcorr2." https://www.mathworks.com/help/signal/ref/xcorr2.html (accessed May 13, 2020).

[37] "Lambert sCMOS," *Lambert Instruments*. https://www.lambertinstruments.com/scmos (accessed May 10, 2020).

[38] "Multispectral image," *Wikipedia*. May 03, 2020, Accessed: May 10, 2020. [Online].

Available:
https://en.wikipedia.org/w/index.php?title=Multispectral_image&oldid=954622833.

[39] A. Holmer *et al.*, "Oxygenation and perfusion monitoring with a hyperspectral camera system for chemical based tissue analysis of skin and organs," *Physiol. Meas.*, vol. 37, no. 11, pp. 2064–2078, Oct. 2016, doi: 10.1088/0967-3334/37/11/2064.

[40] B. Goodman and MA, "Blood Clots Are Another Dangerous COVID-19 Mystery," *WebMD*. https://www.webmd.com/lung/news/20200424/blood-clots-are-another-dangerous-covid-19-mystery (accessed May 13, 2020).

[41] "Stereo Depth," *Intel® RealSenseᴛᴍ Depth and Tracking Cameras*. https://www.intelrealsense.com/stereo-depth/ (accessed May 14, 2020).

[42] C. Zeng, S. Bird, J. J. Luce, and J. Wang, "A Natural-Rule-Based-Connection (NRBC) Method for River Network Extraction from High-Resolution Imagery," *Remote Sens.*, vol. 7, no. 10, pp. 14055–14078, Oct. 2015, doi: 10.3390/rs71014055.

[43] O. Halimi, D. Raviv, Y. Aflalo, and R. Kimmel, "Chapter 7 - Computable invariants for curves and surfaces," in *Handbook of Numerical Analysis*, vol. 20, R. Kimmel and X.-C. Tai, Eds. Elsevier, 2019, pp. 273–314.

[44] Y. Liang, P. Hu, S. Wang, S. Song, and S. Jiang, "Medial axis extraction algorithm specializing in porous media," *Powder Technol.*, vol. 343, pp. 512–520, Feb. 2019, doi: 10.1016/j.powtec.2018.11.061.

[45] J. A. M. Hernández and P. V. Mieghem, "Classification of graph metrics," 2015.